A quantum advection-diffusion solver using the quantum singular value transform

Gard Olav Helle[1]   Tommaso Benacchio[2]

Anna Bomme Ousager[1]   Jørgen Ellegaard Andersen[1]

[1] Center for Quantum Mathematics, University of Southern Denmark, 5230 Odense, Denmark
[2] Weather Research, Danish Meteorological Institute, 2100 Copenhagen, Denmark

Abstract

We present a quantum algorithm for the simulation of the linear advection-diffusion equation based on block encodings of high order finite-difference operators and the quantum singular value transform. Our complexity analysis shows that the higher order methods significantly reduce the number of gates and qubits required to reach a given accuracy. The theoretical results are supported by numerical simulations of one- and two-dimensional benchmarks.

1 Introduction

Computational fluid dynamics simulates and analyses fluid flow using numerical approximations. This involves solving non-linear partial differential equation, typically some incarnation of the Navier-Stokes equation, and requires vast computational resources. Advanced applications include aerospace and automotive engineering and weather prediction. While state-of-the-art numerical models for the latter have made remarkable progress in the last decades, the feasibility of further upgrades clashes with the reality of energy consumption of high-performance computing facilities based on standard hardware that are ever increasing in size to match the challenge of simulations at higher resolutions [BTB15]. Indeed, significant improvements in efficiency are needed for resolution upgrades in operational weather models [SBW+18]. In addition, extracting performance from legacy models involves large amount of human and economic resources at each upgrade, and the sustainability of a business-as-usual scenario remains unclear. As AI-based workflows emerge that come to the rescue for a number of applications in this area [Bau24], questions remain over their accuracy, for example to simulate weather extremes (e.g. [OM24]) .

1

Quantum computers may provide a new avenue for supplying next-generation efficiency in improved fluid dynamical simulations. Numerous quantum algorithms have been developed for the solution of ordinary and partial differential equations (ODEs and PDEs) [BCOW17, Kro23, CO21, ACL23, BC22]. The archetypal example is the Schrödinger equation, which is known to be efficiently solvable on a quantum computer for several families of Hamiltonians [LC17]. It has been demonstrated that non-unitary dynamics can be effectively simulated in certain cases [LKK+21], but obstacles towards generalization remain. A well-known limitation is the presence of exponential growth or decay in the simulated dynamics. In a quantum computer, this situation must be handled via rescaling and/or post-selection, which is infeasible for complexity theoretic reasons [Aar04].

The prevailing approach to simulating PDEs and ODEs is to discretize the problem into a linear system, using finite-difference, finite element, finite volume or spectral methods, which is then solved using a state-of-the-art quantum linear systems algorithm [HHL09, CKS15, GSLW19]. Many time-dependent PDEs can be transformed into a system of ODEs by discretizing the spatial domain, which can then be solved using specialized quantum algorithms. This is the strategy adopted in this work. Due to the linear nature of quantum computers, non-linear equations must be handled through some notion of linearization scheme. In this direction, the Carleman linearization method has been extensively studied [Car32, CSMB25]. The basic idea is to embed the finite dimensional non-linear system into an infinite dimensional linear system, which is then appropriately truncated and solved with an efficient quantum algorithm for linear ODEs.

In this paper, we present a detailed quantum algorithm that implements a numerical solution, based on higher-order finite-difference approximations, to the advection-diffusion equation

$$\partial_t u + c \cdot \nabla u = \nu \Delta u \quad \text{for} \quad u \colon [0, T] \times [0, d]^n \to \mathbb{R}, \tag{1}$$

with periodic boundary conditions, where $c \in \mathbb{R}^n$ is the advection speed, ν is the molecular diffusivity, ∇ is the gradient, and Δ the Laplacian. Our approach is functional; we focus on the one- and two-dimensional cases and give the end-to-end construction in terms of basic one- and two-qubit gates. This results in an easily implementable algorithm that can be tested on current simulators and hardware. The paper is accompanied by a Github repository [HO25] implementing the algorithm with finite-difference approximations of order 2, 4, 6 and 14. The repository also contains functionality for simulating the two-dimensional version of Equation (1).

Several quantum algorithms for the simulation of the advection-diffusion dynamics have been developed before. In [IBP+24] the PDE is reduced to a linear system using low order finite-difference approximations and tackled using the HHL algorithm. The results are also compared with a variational method. A slightly different approach based on low order finite differences and time-marching was studied in [BL24, OBB+25]. More exotic methods have also been considered, e.g. linear combination of Hamiltonian simulation

[NJ24], Schrödingerization [HJLZ24] and probabilistic imaginary time evolution [XWY$^+$24]. In [LKWMK25] the authors are developing explicit circuits for the advection, heat, wave, and Poisson equations based on similar ideas as in the current work, that is, block encoding and quantum singular value transform in Fourier space. To our knowledge, a careful study of the implementation and performance of high order finite-difference operators in this context has not yet been carried out.

To outline our numerical approach, consider for the moment a more general partial differential equation of the form

$$\partial_t u(t, x) = Pu(t, x) \quad u \colon [0, T] \times [0, d]^n \to \mathbb{R}, \tag{2}$$

where P a constant coefficient spatial differential operator. Let L be a finite-difference approximation to P and consider the associated difference-differential equation

$$\dot{v}(t) = Lv(t) \quad \text{for } v \colon [0, T] \to \mathbb{R}^N, \tag{3}$$

where $v(t) \in \mathbb{R}^N$ represents an approximation of $u(t, x)$ on N uniformly distributed grid points. Our approach is to prepare an approximation of the exact solution $v(t) = e^{Lt} v_0$ of (3) using the quantum singular value transform (QSVT) [GSLW19]. To apply this flexible algorithm, we need to construct a so-called unitary block encoding of an operator, say A, which enables us to approximate e^{Lt} as a polynomial in A. For this purpose, we construct unitary block encodings of symmetric finite-difference approximations $D_{2p} \approx \partial_x$ of arbitrary order $2p$ in detail. The basic idea is that any finite-difference operator is a linear combination of translation operators, so an incarnation of the linear combination of unitaries (LCU) method [CW12] can be utilized. The methodology can in principle be applied to construct block-encodings of any finite-difference operator. A generalization to block encodings of pseudo-differential operators is given in [LNY23]. We also establish precise error estimates for the eigenvalues of D_{2p} and the second order analogue $D_{2p}^{(2)}$ (used in both [CO21] and [KWBAG17]) in Theorem 7.2.

For the pure diffusion/heat equation, we propose a new approach using the block encoding of $iD_{2p} \approx i\partial_x$ and QSVT with e^{-Mx^2}, in contrast to the more apparent choice of block encoding $D_{2p}^{(2)} \approx \partial_x^2$ and using QSVT with e^{Mx}. This simplifies the polynomial approximation problem because e^{-Mx^2} is even and bounded by 1 on $[-1, 1]$, thus circumventing scaling issues and the need to use a more comprehensive version of QSVT (see Corollary 3.1.1). The same method is extended in our treatment of the full advection-diffusion equation.

We present a detailed complexity analysis of the one-dimensional algorithm in the form of one- and two-qubit gate counts and qubit requirements. This involves establishing a precise error estimate for the solution of (3) in Theorem 7.4 and a careful estimate of the degree of the polynomial approximations needed to achieve a given precision in the QSVT algorithm. The problem we pose is the following. Given a precision $\epsilon > 0$, an evolution time $T > 0$ and an amplitude encoding of the initial function $u_0(x)$, prepare an amplitude encoding of an

3

approximation of the exact solution u_T of Equation (1) with precision ϵ. In the presence of certain background assumptions on the inputs u_0, ϵ, T, c, ν and p laid out in Section 6, we have the following results. In the pure advection case, $\nu = 0$, our algorithm uses $n + m + 2$ qubits, where

$$n = \lceil \log_2(d(cT||u_0^{(2p+1)}||_{L^2}/\epsilon)^{1/(2p)}) \rceil \qquad \text{and} \qquad m = \lceil \log_2(2p+1) \rceil,$$

and has a gate complexity of

$$\tilde{O}\left((cT)^{1+\frac{1}{2p}} ||u_0^{(2p+1)}||_{L^2}^{\frac{1}{2p}} \log_2(p)^2 \epsilon^{-\frac{1}{2p}} \right). \tag{4}$$

Here, $2p$ is the order of the finite-difference approximation used. In the pure diffusion case, $c = 0$, we use $n + m + 1$ qubits, m is given as above while $n = \lceil \log_2(d(\nu T e^{-\nu T \mu'}||u_0^{(2p+2)}||_{L^2}/\epsilon)^{1/(2p)}) \rceil$, and the gate complexity is

$$\tilde{O}\left((\nu T)^{1+\frac{1}{p}} e^{-\nu T \mu'/p} ||u_0^{(2p+2)}||_{L^2}^{\frac{1}{p}} \log_2(p)^3 \epsilon^{-\frac{1}{p}} \right), \tag{5}$$

Here, $\mu' \approx (2\pi/d)^2$ is a constant. The precise background assumptions and complexity statements are given in Theorem 6.4 and Corollary 6.5.1.

The paper is structured as follows. In Section 2 we provide a more detailed account of the advection-diffusion equation and specify the explicit finite-difference approximations we consider in the paper. In Section 3 we provide the necessary background on QSVT and block encodings, and explain how the algorithm is used to implement the numerical solution. Section 4 covers the construction of the relevant block encodings with the corresponding gate complexity. In Sections 5 and 6 we cover the polynomial approximations needed for QSVT and use this to estimate the overall gate complexity, and in section 7 we establish a precise error estimate between the exact and numerical solution of the equation. In section 8, we briefly explain how the one-dimensional algorithm can be used to handle the general multi-dimensional case. Section 9 displays a number of runs of our algorithm and in particular illustrates when and how the higher order methods are superior to their lower order counterparts. Section 10 draws the conclusions and gives an outlook to future work.

2 Exact solutions and finite-difference approximations

Let us now restrict our attention to the one-dimensional advection-diffusion equation

$$\partial_t u + c \partial_x u = \nu \partial_x^2 u \quad \text{for} \quad u \colon [0, T] \times [0, d] \to \mathbb{R} \tag{6}$$

with periodic boundary conditions. The higher dimensional case will be discussed later. For $k \in \mathbb{Z}$ define

$$e_k(x) := e^{i\omega k x} \quad \text{where} \quad \omega = 2\pi/d. \tag{7}$$

If the initial function is expanded in a Fourier series, $u_0(x) = \sum_{k \in \mathbb{Z}} a_k e_k(x)$, then the exact solution of (6) is given by

$$u(t,x) = \sum_{k \in \mathbb{Z}} a_k e^{-\nu \omega^2 k^2 t} e^{-ic\omega k t} e_k(x). \tag{8}$$

Note that u_0 being of class C^1 is sufficient to ensure absolute convergence of the Fourier series.

For the pure advection equation $\partial_t u_t + c \partial_x u = 0$, the exact solution can be expressed more directly as $u(t,x) = u_0(x - ct)$. The exact solution can with little difficulty be encoded in a quantum circuit, but this is not the goal of our study. Instead, the aim is to develop techniques for efficiently encoding numerical methods with a view towards more complex problems.

As explained in the introduction, our strategy is to replace the differential operator $P = -c \partial_x + \nu \partial_x^2$ by a finite-difference approximation. Introduce N uniformly distributed grid points $x_j = j \Delta x$ for $0 \le j < N$ where $\Delta x := d/N$. For ease of notation, set $x_{j+Nk} := x_j$ for $0 \le j < N$ and $k \in \mathbb{Z}$. For $j \in \mathbb{N}$ let δ_j be the symmetric finite difference operator

$$\delta_j f(x) = \frac{f(x + j\Delta x/2) - f(x - j\Delta x/2)}{j\Delta x} \tag{9}$$

Symmetric finite-difference operators for the first and second derivatives of arbitrary orders are given in the following theorem.

Theorem 2.1. *For $p \ge 1$ the following finite difference operators*

$$D_{2p} := \sum_{j=1}^{p} \alpha_j \delta_{2j} \quad and \quad D_{2p}^{(2)} := \alpha_j \delta_j^2 \quad where \quad \alpha_j = \frac{2(-1)^{j+1}(p!)^2}{(p+j)!(p-j)!}$$

are accurate of order $2p$. More precisely, there are constants C and C' such that for all f of class C^{2p+1} and g of class C^{2p+2} one has

$$|f'(x) - D_{2p}f(x)| \le C||f^{(2p+1)}||_{\infty,[x-p\Delta x, x+p\Delta x]}(\Delta x)^{2p}$$

$$|g''(x) - D_{2p}^{(2p)}f(x)| \le C'||f^{(2p+2)}||_{\infty,[x-p\Delta x, x+p\Delta x]}(\Delta x)^{2p}$$

for all x for which $[x - p\Delta x, x + p\Delta x]$ is contained in the domain of f and g, respectively.

Remark. *The formulas are the result of replacing f by its Lagrange interpolation polynomial at the adjacent grid points $x + j\Delta x$ for $-p \le j \le p$, differentiating and evaluating the result at x. Further proof details are omitted, since the estimates are not explicitly used. Instead, a closely related result is established in Theorem 7.2.*

For an integer $p \ge 1$, we will consider the following two finite difference approximations

$$L = -cD_{2p} + \nu D_{2p}^2 \quad and \quad L = -cD_{2p} + \nu D_{2p}^{(2)} \tag{10}$$

of $P = -c\partial_x + \nu\partial_x^2$, both of order $2p$. The second is perhaps the most natural choice from a numerical perspective, but the first choice is more convenient from a quantum computational perspective. We will elaborate on this point in the next section.

3   The Quantum Singular Value Transform

Throughout the paper, let $H_n := \mathbb{C}^{2^n}$, $n \geq 1$, denote the n-qubit Hilbert space and $\{|k\rangle : 0 \leq k < 2^n\}$ the computational basis. The isomorphisms $(\mathbb{C}^2)^{\otimes n} \cong \mathbb{C}^{2^n}$ are specified by the least significant bit first convention, that is,

$$|j_0\rangle |j_1\rangle \cdots |j_{n-1}\rangle \mapsto |j\rangle \quad \text{where } j := \sum_{s=0}^{n-1} j_s 2^s.$$

We follow the standard conventions on quantum gates and circuits given in [NC10, chap. 4] unless otherwise stated. In particular, the standard Pauli gates are denoted by X, Y, Z and the Hadamard gate is denoted by H.

Our quantum algorithm is based on the quantum singular value transform (QSVT) [GSLW19], a joint generalization of quantum signal processing and qubitization [LYC16, LC16]. In order to state the relevant results, we need to recall some terminology. Let $A \colon H_k \to H_k$ be a linear map. A unitary block encoding of A is a pair

$$(\iota \colon H_k \to H_n, U \colon H_n \to H_n),$$

where ι is an isometry and U is a unitary such that $A = \iota^\dagger \circ U \circ \iota \colon H_k \to H_k$. A block encoding of A exists if and only if $||A|| := \sup_{x \,:\, ||x|| \leq 1} ||Ax|| \leq 1$. If this condition is not met, one must work with a scaled version A/α and keep track of the scaling factor α.

Remark. *In [GSLW19] the authors work with $V := \operatorname{Im} \iota \subset H_n$ and the internal projection $\Pi := \iota \circ \iota^\dagger \colon H_n \to H_n$ in place of H_k and ι. They also work with a more general notion of block encoding for linear maps $A \colon H_k \to H_m$, which is unnecessary for our purpose.*

The form in which we apply the algorithm is stated in the following theorem.

Theorem 3.1. *Let $(\iota \colon H_k \to H_n, U \colon H_n \to H_n)$ be a unitary block encoding of a Hermitian operator $A \colon H_k \to H_k$ and let $q \in \mathbb{R}[x]$ be an even or odd polynomial of degree d satisfying $|q(x)| \leq 1$ for all $x \in [-1, 1]$. Then there exists an angle sequence (depending only on q) $\Phi = (\phi_1, \phi_2, \cdots, \phi_d)$ such that*

$$(U_\Phi \colon H_1 \otimes H_n \to H_1 \otimes H_n, |0\rangle \otimes \iota \colon H_k \to H_1 \otimes H_n)$$

defines a block encoding of $q(A) \colon H_k \to H_k$, where U_Φ is defined by the quantum circuit in Figure 1. The resources required for the circuit are given by

(1) d applications of U or $U^\dagger$,

(2) $2d$ applications of $C_\Pi \,\mathrm{NOT} \coloneqq X \otimes \Pi + I \otimes (I - \Pi)$ and
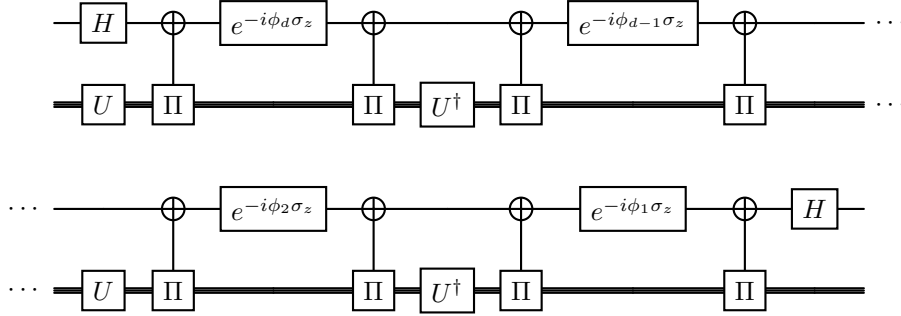
(3) $(d+2)$ 1-qubit gates.

Figure 1: The quantum circuit U_Φ for an angle sequence $\Phi = (\phi_1, \cdots, \phi_d)$ with d even.

Remark. *We make some clarifications. For a detailed account of the above theorem and its proof, the reader should consult the original reference [GSLW19].*

- *The theorem remains true if A is not Hermitian, but then we must apply q to A in the singular value sense defined in [GSLW19, def. 16].*

- *The theory explaining the relation between angle sequences and polynomials is called quantum signal processing (QSP). In the above form, the angle sequence associated with a given polynomial is not unique.*

- *An efficient and numerically stable way to compute the angle sequence associated with a given polynomial is given in [DMWL21] with a corresponding MATLAB package QSPACK. Their method is also implemented in the python package pyqsp introduced in [MRTC21].*

The most common choice of isometry is $\iota \colon |0\rangle \otimes I \colon H_k \to H_a \otimes H_k \cong H_{k+a}$, in which case, $\Pi = |0\rangle \langle 0| \otimes I$ and the $C_\Pi \,\mathrm{NOT}$ gate is simply a multi-controlled NOT gate with control state $|0\rangle \in H_a$. To keep the gate count low, it is therefore important to keep the number a of ancilla qubits to a minimum.

By introducing an additional ancilla qubit and applying Theorem 3.1 for two angle sequences in parallel, polynomials without definite parity [GSLW19, Thm. 56] can be handled. A precise statement is contained in the following corollary.

Corollary 3.1.1. *Let $(\iota \colon H_k \to H_n, U \colon H_n \to H_n)$ be a unitary block-encoding of a Hermitian operator $A \colon H_k \to H_k$ and let $q \in \mathbb{R}[x]$ be a polynomial of degree $d+1$ satisfying $|q(x)| \le 1$ for all $x \in [-1,1]$. Let $q(x) = q_1(x) + q_2(x)$ be the*

decomposition of q into even and odd parts, where we take q_2 to have a greater degree than q_1. Let

$$\Phi^{(1)} = (\phi_1^{(1)}, \cdots, \phi_d^{(1)}) \quad and \quad \Phi^{(2)} = (\phi_1^{(2)}, \cdots, \phi_d^{(2)}, \phi_{d+1}^{(2)})$$

be angle sequences associated with q_1 and q_2, respectively, as given in Theorem 3.1. Then

$$(U_{(\Phi^{(1)}, \Phi^{(2)})} \colon H_1^{\otimes 2} \otimes H_n \to H_1^{\otimes 2} \otimes H_n, \; |0\rangle^{\otimes 2} \otimes \iota \colon H_k \to H_1^{\otimes 2} \otimes H_n)$$

defines a block encoding of $(1/2)q(A) \colon H_k \to H_k$, where $U_{(\Phi^{(1)}, \Phi^{(2)})}$ is defined by the quantum circuit in Figure 2. The resources required for the circuit are

(1) d applications of U or $U^\dagger$,

(2) one application of controlled U (or $U^\dagger$),

(3) $2(d+1)$ applications of C_Π NOT,
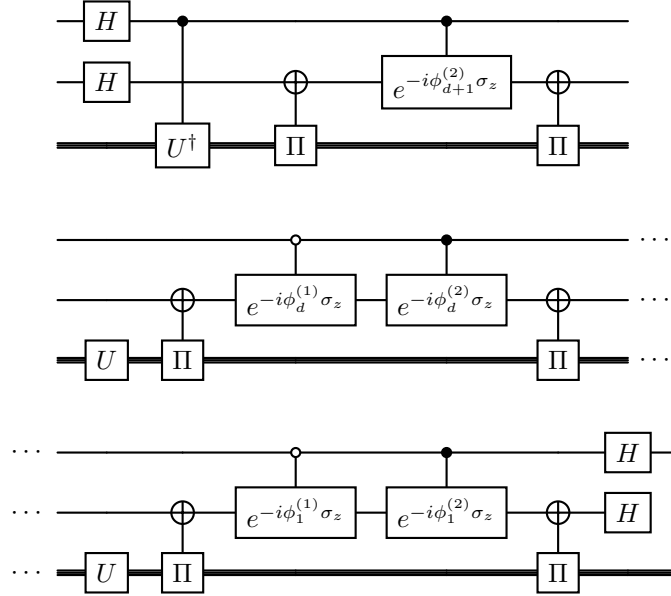
(4) $(2d+1)$ 2-qubit gates and 4 1-qubit gates.

Figure 2: The quantum circuit $U_{(\Phi^{(1)}, \Phi^{(2)})}$ for a pair of angle sequences $\Phi^{(1)} = (\phi_1^{(1)}, \ldots, \phi_d^{(1)})$ and $(\Phi^{(2)} = (\phi_1^{(2)}, \ldots, \phi_{d+1}^{(2)})$ with d odd.

Remark. *To construct the linear combination $q_1(x) + iq_2(x)$ instead of $q_1(x) + q_2(x)$ as in Corollary 3.1.1, it suffices to add an initial gate $S = |0\rangle \langle 0| + i |1\rangle \langle 1|$ to the first qubit in Figure 2.*

Let us now explain how we can implement our approximate numerical solution $e^{Lt}v_0$ with the aid of QSVT for the two choices of L given in (10). Consider first $L = -cD_{2p} + \nu D_{2p}^2$. Since L is a polynomial in D_{2p}, the idea is to block encode the Hermitian matrix $H = i\beta D_{2p}$, for a normalizing constant β that ensures $||H|| \leq 1$, and apply QSVT as in Corollary 3.1.1 with q a polynomial approximation of the function

$$f(x; M_1, M_2) = e^{-M_1 x^2 + iM_2 x} = e^{-M_1 x^2} \cos(M_2 x) + ie^{-M_1 x^2} \sin(M_1 x), \quad (11)$$
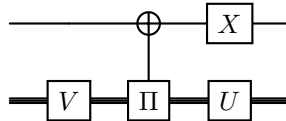
where $M_1 = cT/\beta$ and $M_2 = \nu T/\beta^2$. The constant β will be specified later. Both the real and imaginary part of $f(x; M_1, M_2)$ is bounded by 1 one $[-1, 1]$ and a polynomial approximation to any desired precision can be constructed explicitly as we show later in Proposition 5.5. Note that in the pure advection case, $\nu = 0$, we are in the situation of a Hamiltonian simulation problem.

Consider now the second choice $L = -cD_{2p} + \nu D_{2p}^{(2)}$, and let $S = \nu D_{2p}^{(2)}$ and $H = icD_{2p}$. Then S and H are commuting Hermitian operators, so in particular $e^{LT} = e^{ST}e^{iHT}$. Here, both factors can be implemented via QSVT in the form of Corollary 3.1.1 given access to block encodings of normalized versions of S and H. The second factor is a Hamiltonian simulation problem and does not offer much difficulty. The first factor is slightly more difficult to deal with for the following reason. S has a non-positive spectrum (this will be shown later, see Eq. (38)) containing 0, and the function we seek to apply is $x \mapsto e^{Tx}$, which is not bounded by 1 for positive x. Therefore, one must choose a polynomial that approximates e^{Tx} on $[-1, 0]$ and is bounded by 1 on $[0, 1]$. Here, a numerical approximation approach seems to be superior to analytic methods. For instance, the even extension $x \mapsto e^{-T|x|}$ is problematic due to the lack of smoothness at zero leading to artificially high degree polynomial approximations. Finally, the two block encodings of e^{ST} and e^{iHT} must be composed to produce a block encoding of the desired operator. This can be achieved with the following basic lemma. The construction is given in [DMB$^+$25, sec. 10.2] and we include a short proof.

Lemma 3.2. *Suppose that $U, V \colon H_n \to H_n$ are unitary block encodings of*

$$A, B \colon \operatorname{Im}\Pi \to \operatorname{Im}\Pi,$$

respectively, for an orthogonal projection $\Pi \colon H_n \to H_n$. Then the following quantum circuit specifies a unitary block encoding $W \colon H_1 \otimes H_n \to H_1 \otimes H_n$ of the composition AB on the subspace $|0\rangle \otimes \operatorname{Im}\Pi$

Proof. Let $|\psi\rangle$ be a state in $\operatorname{Im}\Pi$. Then, by the definition of block encoding, we can write

$$V|\psi\rangle = B|\psi\rangle + |g\rangle \quad \text{and} \quad U(B|\psi\rangle) = A(B|\psi\rangle) + |g'\rangle$$

for a pair of unimportant garbage states $|g\rangle, |g'\rangle \in \operatorname{Ker}\Pi = \operatorname{Im}\Pi^{\perp}$. The effect of the above circuit on $|0\rangle|\psi\rangle$ is therefore

$$(X \otimes U)(|1\rangle B|\psi\rangle + |0\rangle|g\rangle) = |0\rangle AB|\psi\rangle + |0\rangle|g'\rangle + |1\rangle U|g\rangle.$$

The orthogonal projection of this state on the subspace $|0\rangle \otimes \operatorname{Im}\Pi$ is precisely $|0\rangle AB|\psi\rangle$ as desired. $\qquad\square$

In conclusion, the second method requires two different block encodings instead of one, both factors require the use of QSVT in the form of Corollary 3.1.1 leading to a scaling factor of $(1/2)^2 = 1/4$ instead of $1/2$, and the composition introduces an additional ancilla qubit. Moreover, the first approach leads to a much more natural approximation problem within the QSVT framework, since $e^{-M_1 x^2}$ is even and bounded by 1 for $x \in [-1, 1]$ in contrast to $e^{M_2 x}$. For these reasons, we find the first approach to be superior.

Remark. *In principle, amplitude amplification [GSLW19, Thm. 27] can be used to increase the success probability of a quantum circuit. However, this can be expensive and simply not accessible without efficient access to a reflection operator in the initial state, which is not assumed in our situation.*

4 Block encoding of finite-difference operators

In order to apply the QSVT algorithm as outlined in the previous section, we need to construct efficient block encodings of the finite difference operators D_{2p} and $D_{2p}^{(2)}$ for positive integers p. These operators are linear combinations of the basic finite difference operators δ_{2j}, $j \geq 1$, which in turn are linear combinations of translation operators (see Theorem 2.1 and Equation (9) for the definitions). Since we work in a periodic domain, the matrices we seek to block encode are therefore circulant and sparse. Efficient block encoding strategies for circulant matrices have been known for some time [ZW17] (see also the more recent [CLVBY24] and [MW24, Sec. V]). The basic idea is to use a modular adder [Dra00] and the linear combinations of unitaries (LCU) method originally introduced in [CW12].

In the following, we lay out the details of our block encoding of D_{2p}, tailor-made for the application at hand, with corresponding gate complexities, by which we mean the number of 2-qubit gates (2Q-gates) and 1-qubit gates (1Q-gates). In fact, the only 2Q-gates employed are controlled 1Q-gates. Minor modifications of the construction presented result in block encodings of the operators $D_{2p}^{(2)}$ as well. More generally, the methods can be applied to block encode finite-difference operators in any dimension.

In the following, it will be convenient to extend the notation $|k\rangle \in H_n$ to all $k \in \mathbb{Z}$ under the convention that $|k\rangle = |l\rangle$ if and only if $k \equiv l \mod 2^n$.

Definition 4.1. *Define $T \in U(H_n)$ to be the translation operator given by $T|k\rangle = |k+1\rangle$ for all $k \in \mathbb{Z}$.*

Note that T has order $N = 2^n$ so that $T^{-1} = T^{N-1}$. Now, as operators on H_n we have

$$\delta_{2j} = \frac{1}{2j\Delta x}(T^j - T^{-j}) \quad \text{and} \quad \delta_j^2 = \frac{1}{(j\Delta x)^2}(T^j - 2I + T^{-j}). \qquad (12)$$

More generally, any linear combination of these operators can be expressed as a polynomial in T. The circulant matrices are precisely the polynomials in T.

Remark. *The circulant matrices is typically defined as the centralizer $C(T) = \{A\colon H_n \to H_n\colon AT = TA\}$. For $A \in C(T)$, let $A\,|0\rangle = \sum_{j=0}^{N-1} a_j\,|j\rangle$. One can then verify that $A = \sum_{j=0}^{N-1} a_j T^j$ by checking the action on the computational basis. Thus $C(T) = \mathbb{C}[T] \subset \mathrm{End}(H_n)$, showing that the circulant matrices coincide with the commutative algebra of polynomials in T.*

A modular adder is simply the unitary obtained by encoding the powers of the translation operator in parallel. The following more flexible version is appropriate for our purpose.

Definition 4.2. *For integers $n, m, l \in \mathbb{Z}$ with $n \geq m \geq 1$ define the modular adder $M_{m,n,l}\colon H_m \otimes H_n \to H_m \otimes H_n$ by the rule*

$$M_{m,n,l}\,|j\rangle\,|k\rangle = |j\rangle\,T^{j+l}\,|k\rangle = |j\rangle\,|k + j + l\rangle \quad j, k \in \mathbb{Z}.$$

The modular adder is diagonalized by the Fourier transform on the second registry.

Lemma 4.3. *Define $R \in \mathrm{End}(H_n)$ to be the diagonal operator given by $R\,|k\rangle = e^{2\pi i k/N}\,|k\rangle$ for $0 \leq k < N$, where $N = 2^n$. Then $T = \mathcal{F}^{-1}R\mathcal{F}$, where $\mathcal{F}$ is the quantum Fourier transform given by*

$$\mathcal{F}\,|k\rangle = 2^{-n/2} \sum_{j=0}^{N-1} e^{2\pi i j k/N}\,|j\rangle \quad \text{for } 0 \leq k < N. \qquad (13)$$

Proof. It suffices to observe that $T\hat{e}_k = e^{2\pi i k/N}\hat{e}_k$, where $\hat{e}_k = \mathcal{F}^{-1}\,|k\rangle = 2^{-n/2}\sum_{j=0}^{N-1} e^{-2\pi i j k/N}\,|j\rangle$, for $0 \leq k < N$. $\qquad\square$

In view of the above result, we introduce what we coin the phase adder

$$P_{m,n,l} := (1 \otimes \mathcal{F})M_{m,n,l}(1 \otimes \mathcal{F}^{-1}) = \sum_{j=0}^{2^m-1} |j\rangle\,\langle j| \otimes R^{j+l}. \qquad (14)$$

The phase adder admits a simple quantum circuit implementation using similar ideas as in the well-known quantum circuit implementation of the quantum Fourier transform.

Write $P_{m,n} = P_{m,n,0}$ and observe that $P_{m,n,l} = (1 \otimes R^l) \circ P_{m,n}$. We have

$$R^l = \bigotimes_{s=0}^{n-1} P(2\pi l/2^{n-s}) \quad \text{where} \quad P(\theta) = \begin{pmatrix} 1 & 0 \\ 0 & e^{i\theta} \end{pmatrix} \quad \text{for } \theta \in \mathbb{R}. \qquad (15)$$

Let $CP_{s,t}(\theta)\colon H_m \otimes H_n \to H_m \otimes H_n$ denote the controlled phase gate with control and target specified by $0 \le s < m$ and $0 \le t < n$. Explicitly,

$$CP_{s,t}(\theta)\,|j\rangle\,|k\rangle = e^{i\theta j_s k_t}\,|j\rangle\,|k\rangle \qquad \text{for } 0 \le j < 2^m,\ 0 \le k < 2^n. \qquad (16)$$

Proposition 4.4. *The phase adder $P_{m,n}$ can be implemented with $O(mn)$ 2Q-gates as follows*

$$P_{m,n} = \prod_{s=0}^{m-1}\left(\prod_{t=0}^{n-s-1} CP_{s,t}(2\pi/2^{n-s-t})\right),$$

where the product denotes gate composition.

Proof. For $0 \le j < 2^m$ and $0 \le k < 2^n$ we compute

$$P_{m,n}\,|j\rangle\,|k\rangle = e^{2\pi jk/2^n}\,|j\rangle\,|k\rangle = \left(\prod_{s=0}^{m-1}\prod_{t=0}^{n-1} e^{2\pi j_s k_t/2^{n-s-t}}\right)|j\rangle\,|k\rangle$$

$$= \left(\prod_{s=0}^{m-1}\prod_{t=0}^{n-s-1} e^{2\pi j_s k_t/2^{n-s-t}}\right)|j\rangle\,|k\rangle$$

$$= \prod_{s=0}^{m-1}\left(\prod_{t=0}^{n-s-1} CP_{s,t}(2\pi/2^{n-s-t})\right)|j\rangle\,|k\rangle,$$

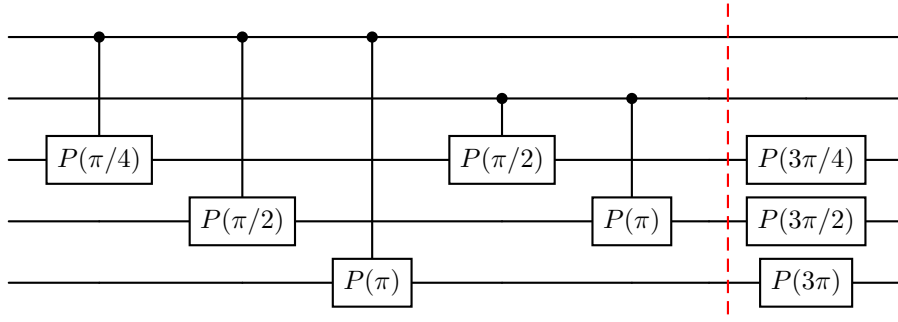which establishes the required formula. The number of 2Q-gates is given by

$$\sum_{s=0}^{m-1}(n-s) = nm - \sum_{s=0}^{m-1} s = nm - m(m-1)/2 = O(mn).$$

$\square$

Remark. *The $CP_{s,t}(\theta)$ gates are all diagonal in the computational basis, so the order of the factors is irrelevant.*

Example 1. *The quantum circuit for $P_{2,3,3} = R_3 \circ P_{2,3}$ takes the following form.*

Corollary 4.4.1. *Let $n \geq m \geq 1$ and $l \in \mathbb{Z}$.*

(i) *The phase adder $P_{n,m,l}$ can be implemented with $O(mn)$ 2Q-gates and $O(n)$ 1Q-gates.*

(ii) *The modular adder $M_{n,m,l}$ can be implemented with $O(n^2)$ 2Q-gates and $O(n)$ 1Q-gates.*

Proof. We have $P_{n,m,l} = (1 \otimes R^l) \circ P_{n,m}$. The first factor requires $O(n)$ 1Q-gates, and the second factor requires $O(mn)$ 2Q-gates according to Proposition 4.4.

The modular adder $H_{n,m,l}$ is obtained from $P_{n,m,l}$ by conjugation with the Fourier transform in the second registry as in equation (14). The Fourier transform requires $O(n^2)$ 2Q-gates, which dominates the 2Q-gate count of $P_{m,n,l}$ as $m \leq n$, resulting in the stated estimate. □

The LCU method first introduced in [CW12] can be stated in the following form.

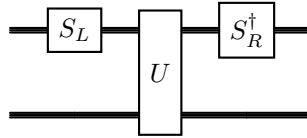**Lemma 4.5.** *Let $m, n \in \mathbb{N}$ and let $S_L, S_R \in U(H_m)$ be a pair satisfying*

$$S_L \left| 0 \right\rangle = \sum_{j=0}^{2^m - 1} b_j \left| j \right\rangle \quad and \quad S_R \left| 0 \right\rangle = \sum_{j=0}^{2^m - 1} c_j \left| j \right\rangle .$$

Let $\{U_j \in U(H_n)\}_{j=0}^{2^m - 1}$ be a family of unitaries and set

$$U = \sum_{j=0}^{2^m - 1} \left| j \right\rangle \left\langle j \right| \otimes U_j \in U(H_m \otimes H_n).$$

Then the following circuit defines a block encoding of $A := \sum_{j=0}^{2^m - 1} a_j U_j$ on the subspace $\left| 0 \right\rangle \otimes H_n \subset H_m \otimes H_n$, where $a_j = b_j \bar{c}_j$ for $0 \leq j < 2^m$.

The pair $(S_L, S_R) \in U(H_m)$ is called a state preparation pair for the vector $a = \sum_j a_j \left| j \right\rangle$. Since both $S_L \left| 0 \right\rangle$ and $S_R \left| 0 \right\rangle$ are unit vectors, it follows that

$$||a||_1 = \sum_j |a_j| = \sum_j |b_j||c_j| \leq \frac{1}{2} \sum_j |b_j|^2 + |c_j|^2 = 1 \tag{17}$$

with equality if and only if $|b_j| = |c_j|$ for all j.

Remark. *Note also that $||A|| \leq \sum_j |a_j|||U_j|| = ||a||_1$, but we rarely have equality.*

Let us now consider how to construct a state preparation pair (S_L, S_R) for block encoding $H = i\beta D_{2p}$, where $D_{2p} = \sum_{j=1}^{p} \alpha_j \delta_{2j}$ is given in Theorem [2.1] and β is an appropriate normalizing constant. Since

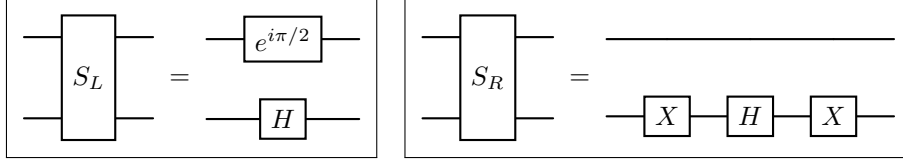$$(\Delta x) D_{2p} = \sum_{j=1}^{p} \frac{\alpha_j}{2j}(T^j - T^{-j}), . \tag{18}$$

we will use the modular adder $M_{m,n,p} = \sum_{j=0}^{2^m-1} |j\rangle \langle j| \otimes T^{j-p}$ with $m := \lceil \log_2(2p+1) \rceil$, combined with a state preparation pair for the vector

$$a = a(p) := i c_p \sum_{j=1}^{p} \frac{\alpha_j}{2j}(|p+j\rangle - |p-j\rangle) \quad \text{where} \quad c_p^{-1} = \sum_{j=1}^{p} \frac{|\alpha_j|}{j}. \tag{19}$$

Here, the normalization ensures that $\|a\|_1 = 1$, which is optimal according to Equation (17). Explicitly, we may take (S_L, S_R) to satisfy

$$S_L |0\rangle = i\sqrt{c_p} \sum_{j=1}^{p} \left(\frac{|\alpha_j|}{2j}\right)^{1/2} (|p+j\rangle + |p-j\rangle) \tag{20}$$

$$S_R |0\rangle = \sqrt{c_p} \sum_{j=1}^{p} (-1)^{j+1} \left(\frac{|\alpha_j|}{2j}\right)^{1/2} (|p+j\rangle - |p-j\rangle).$$

Example 2. *For $p = 1$, we compute $\alpha_1 = 1$ and $c_p = 1$. We seek $S_L |00\rangle = \frac{i}{\sqrt{2}}(|00\rangle + |01\rangle)$ and $S_R |00\rangle = \frac{1}{\sqrt{2}}(-|00\rangle + |01\rangle)$. We may take*

It is possible to reduce the ancilla count in the block encoding to one, but this is special to $p = 1$.

Example 3. *For $p = 3$, we compute $(\alpha_1, \alpha_2, \alpha_3) = (3/2, -3/5, 1/10)$ and $c_3 = 6/11$. The vector we want to prepare is*

$$a = i\left[\frac{1}{110}(|0\rangle - |6\rangle) - \frac{9}{110}(|1\rangle - |5\rangle) - \frac{9}{22}(|2\rangle - |4\rangle)\right].$$
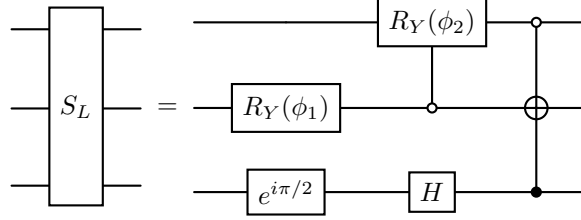
By the above recipe, we then seek (S_L, S_R) satisfying

$$S_L |000\rangle = i\left[u(|010\rangle + |001\rangle) + v(|100\rangle + |101\rangle) + w(|000\rangle + |011\rangle)\right]$$
$$S_R |000\rangle = \left[u(-|010\rangle + |001\rangle) + v(|100\rangle - |101\rangle) + w(-|000\rangle + |011\rangle)\right],$$

for $(u, v, w) = (\sqrt{9/22}, \sqrt{9/110}, \sqrt{1/110})$. *Set* $\phi_1 = \arcsin(\sqrt{9/11})$ *and* $\phi_2 = \arcsin(\sqrt{9/10})$ *and let*
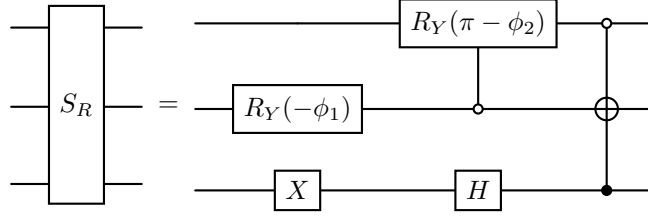
$$R_Y(\theta) = \begin{pmatrix} \cos(\theta) & -\sin(\theta) \\ \sin(\theta) & \cos(\theta) \end{pmatrix}.$$
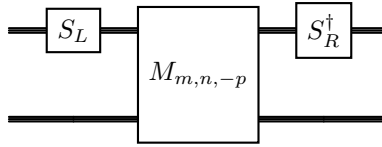
Then

does the trick. The two upper rotation gates prepare $\sqrt{2}(w\,|0\rangle + v\,|1\rangle + u\,|2\rangle)$, *and from here it is clear how one arrives at the desired vector.*

Some minor modifications are needed to account for the signs needed for S_R.

Theorem 4.6. *Let* $p \geq 1$ *be an integer and set* $m = \lceil \log_2(2p+1) \rceil$. *Let* (S_L, S_R) *be a state preparation pair satisfying* (20). *The quantum circuit*
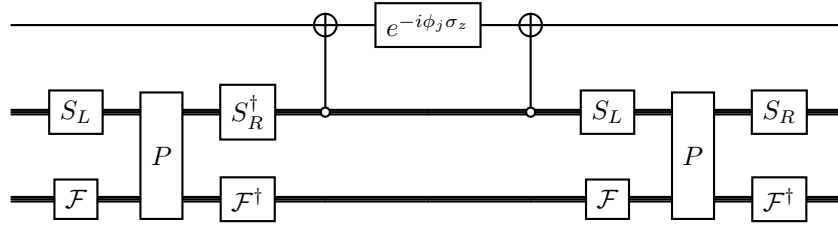

defines a unitary block encoding of the Hermitian matrix $H := i(c_p \Delta x) D_{2p}$ *on the subspace* $|0\rangle \otimes H_n \subset H_m \otimes H_n$, *where* c_p *is defined in* (19). *The resources used are* $O(p)$ *2Q- and 1Q-gates for* S_L *and* S_R, $O(n^2)$ *2Q-gates and* $O(n)$ *1Q-gates for* $M_{m,n,-p}$.

Proof. The fact that the quantum circuit defines the required block encoding of H follows by unpacking the various definitions and applying Lemma 4.5. For the complexity statement, note that $M_{m,n,-p}$ is implemented with $O(n^2)$ 2Q-gates and $O(n)$ 1Q-gates by Corollary 4.4.1. General state preparation on m qubits has complexity $\Theta(2^m)$ in size [STY+21]. As $m = \lceil \log_2(2p+1) \rceil$, this leads to a gate complexity of $O(2^m) = O(p)$ 2Q- and 1Q-gates for S_L and S_R. □

The dominant resource cost of the above block encoding is due to the conjugation by the quantum Fourier transform in the modular adder. When this block encoding is used in the QSVT circuit (see Figure 1 or 2), all of these gates will cancel except for a single initial and terminal application.

Example 4. *An excerpt of the QSVT circuit with the above block encoding. Here $P = P_{m,n,-p}$.*

Clearly, the middle $\mathcal{F}$ and $\mathcal{F}^\dagger$ in the lower register are superfluous.
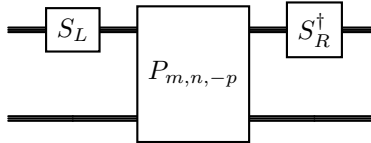
More formally, we have the following observation, whose proof is essentially contained in the above example and therefore omitted.

Lemma 4.7. *Let $\mathrm{QSVT}(U, \Pi, \Phi)$ be the QSVT circuit of Theorem 3.1 associated with a unitary block encoding U, orthogonal projection Π and angle sequence Φ. If $U = FVF^\dagger$ for a unitary F commuting with Π, then*

$$\mathrm{QSVT}(U, \Pi, \Phi) = (I \otimes F)\,\mathrm{QSVT}(V, \Pi, \Phi)(I \otimes F^\dagger).$$

An analogous result is true for the QSVT version of Corollary 3.1.1. The block encoding of primary relevance in our application is therefore obtained by replacing the modular adder with the phase adder.

Theorem 4.8. *Let $p \geq 1$ be an integer and set $m = \lceil \log_2(2p+1) \rceil$. Let (S_L, S_R) be a state preparation pair satisfying (20). The following quantum circuit*

defines a unitary block encoding of the Hermitian matrix $H := i(c_p \Delta x)\mathcal{F}^\dagger D_{2p}\mathcal{F}$ on the subspace $|0\rangle \otimes H_n \subset H_m \otimes H_n$, where c_p is defined in (19) and $\mathcal{F}$ is the quantum Fourier transform. The resources used are $O(p)$ 2Q- and 1Q-gates for S_L and S_R, $O(mn)$ 2Q-gates and $O(n)$ 1Q-gates for $P_{m,n,-p}$.

For later reference, we provide the complexity of applying QSVT with the above block encoding.

Lemma 4.9. *Let U be the block encoding of Theorem 4.8 using $m + n$ qubits with $m = \lceil \log_2(2p+1) \rceil$. The resources required to apply QSVT in the form of Corollary 3.1.1 with the block encoding U and a polynomial of degree $d+1$ are $2 + m + n$ qubits and $O(dmn)$ 2Q and 1Q gates.*

Proof. It is clear that the circuit uses $2 + m + n$ qubits. We estimate the gate count for each item in the resource overview given in Corollary 3.1.1 as follows.

(i) d applications of U or $U^\dagger$ uses $O(dmn)$ 2Q-gates and $O(dn)$ 1Q-gates.

(ii) An application of controlled U (or $U^\dagger$) can naively be implemented by putting controls on all the 2Q- and 1Q-gates involved. A doubly controlled 1Q-gate, say $C^2 V$, can be realized with two CNOT gates, two $C\sqrt{V}$ gates and one $C\sqrt{V}^\dagger$ gate by a standard construction [BBC$^+$95]. Since all of the 2Q-gates in our construction can be taken to be of this form, CU can be realized with $O(mn)$ gates.

(iii) $2(d+1)$ applications of $C_\Pi \text{NOT}$. In our case $\Pi = |0\rangle \langle 0| \otimes I_{H_n}$. Therefore, $C_\Pi \text{NOT} = C^m \text{NOT}$ with control state $0 = [0 \cdots 0]_2$, which can be implemented with $O(m^2)$ gates without ancillas [BBC$^+$95] (with ancillas the complexity can be reduced to $O(m)$). The total cost of this item is therefore $O(m^2 d)$.

(iv) $(2d+1)$ 2Q-gates and 4 1Q-gates has complexity $O(d)$.

(v) Finally, we also have to include a conjugation by the quantum Fourier transform on the n-qubit registry. This has complexity $O(n^2)$ (see Lemma 4.7).

Since we require $m < n$, the resources are dominated by the first item, leading to a total complexity of $O(dmn)$. $\qquad\square$

5 Polynomial approximations

In order to estimate the overall complexity of our quantum algorithm, we need to estimate the degree of the polynomial approximation needed to match the desired function to a given precision. Recall that the function of interest is (see Eq. 11)

$$f(x; M_1, M_2) = e^{-M_1 x^2 + M_2 i x} \quad \text{for} \quad M_1, M_2 \in \mathbb{R}_{\geq 0}. \tag{21}$$

For computational purposes, it is also ideal to have specific expressions for the polynomials in the Chebyshev basis. The corresponding angle sequences can then be accurately computed with the method of [DMWL21].

The function $f(x; 0, M)$ is the key function for Hamiltonian simulation and the necessary approximation results are contained in [GSLW19, sec. 5.1], [LC16, LC17]. In the following, we present the relevant results and establish an appropriate generalization to $f(x; M_1, M_2)$.

For $z \in \mathbb{C}$ and $\theta \in \mathbb{R}$ one has the Jacobi-Anger expansion

$$e^{iz\cos(\theta)} = J_0(z) + 2\sum_{n=1}^{\infty} i^n J_n(z)\cos(n\theta), \tag{22}$$

where $J_n(z)$ is the n'th Bessel function of the first kind [AS64]. This leads to the Chebyshev expansion

$$e^{izx} = J_0(z) + 2\sum_{n=1}^{\infty} i^n J_n(z)T_n(x), \quad x \in [-1,1], \tag{23}$$

where $T_n(x)$ is the n'th Chebyshev polynomial of the first kind specified by $T_n(\cos(\theta)) = \cos(n\theta)$. By equating real and imaginary parts, one obtains the Chebyshev expansions of $\cos(Mx)$ and $\sin(Mx)$. Introduce the corresponding truncations

$$C_R(x;M) = J_0(M) + \sum_{k=1}^{R}(-1)^k J_{2k}(M)T_{2k}(x) \tag{24}$$

$$S_R(x;M) = \sum_{k=0}^{R}(-1)^k J_{2k+1}(M)T_{2k+1}(x).$$

The following result of [GSLW19, Lemma 57] provides an upper bound for the truncation degree needed to achieve a given accuracy. To state the result, we need the following definition.

Definition 5.1. *For $\epsilon \in (0,1)$ and $M > 0$, let $r(M,\epsilon) \in (M, \infty)$ be defined implicitly by the formula*
$$(M/r)^r = \epsilon.$$

Lemma 5.2. *Given $M > 0$ and $\epsilon \in (0,1)$ define $R := \lfloor \frac{1}{2}r(eM/2, 5\epsilon/4)\rfloor$. Then*

$$|C_R(x;M) - \cos(Mx)| \le \epsilon \quad \text{and} \quad |S_R(x;M) - \sin(Mx)| \le \epsilon$$

for all $x \in [-1,1]$.

We will derive a similar bound for $g(x;M) = e^{-Mx^2}$.

Lemma 5.3. *We have the following Chebyshev expansion*

$$e^{-Mx^2} = e^{-M/2}J_0(iM/2) + 2e^{-M/2}\sum_{n=1}^{\infty} i^n J_n(iM/2)T_{2n}(x) \tag{25}$$

for $x \in [-1,1]$.

Proof. Replace θ by 2θ and z by $iM/2$ in the Jacobi-Anger expansion in Equation (22) to arrive at the given formula. $\square$

Let $E_R(x;M)$ denote the degree $2R$ truncation of the series (25).

Lemma 5.4. *Given $\epsilon > 0$ and $M > 0$, set $R = \lfloor r(eM/4, 5\epsilon/6) \rfloor$. Then*

$$|e^{-Mx^2} - E_R(x; M)| \leq \epsilon \quad \text{for } x \in [-1, 1].$$

Proof. For $x \in [-1, 1]$ we have

$$|e^{-Mx^2} - E_R(x; M)| = 2 \left| \sum_{k=R+1}^{\infty} i^k e^{-M/2} J_k(iM/2) T_{2k}(x) \right|$$

$$\leq 2 \sum_{k=R+1}^{\infty} e^{-M/2} |J_k(iM/2)|$$

By [AS64, 9.1.62], we have the bound $|J_k(iM/2)| \leq e^{M/2}(M/4)^k/k!$, so that

$$2 \sum_{k=R+1}^{\infty} e^{-M/2} |J_k(iM/2)| \leq 2 \sum_{k=R+1}^{\infty} \frac{(M/4)^k}{k!} \leq 2 \frac{(M/4)^{R+1}}{(R+1)!} \sum_{l=0}^{\infty} (1/2)^l$$

$$= 4 \frac{(M/4)^{R+1}}{(R+1)!} \leq \frac{4}{\sqrt{2\pi(R+1)}} \left(\frac{Me}{4(R+1)} \right)^{R+1},$$

where we have used that $R \geq M/2$ in the second inequality and Stirling's formula $n! \geq \sqrt{2\pi n}(n/e)^n$ in the final inequality. From $R = \lfloor r(eM/4, 5\epsilon/6) \rfloor$, it follows that $R + 1 \geq r(eM/4, 5\epsilon/6)$. Therefore,

$$\frac{4}{\sqrt{2\pi(R+1)}} \left(\frac{Me}{4(R+1)} \right)^{R+1} \leq \frac{6}{5} \left(\frac{Me}{4(R+1)} \right)^{R+1} \leq \frac{6}{5} \left(\frac{Me}{4r} \right)^r = \epsilon.$$

as desired. $\square$

Remark. *The method of truncating the Chebyshev series of an analytic function tends to yield good uniform estimates on $[-1, 1]$. In fact, in the above situation, one can show that the method leads to optimal asymptotic estimates [AA22].*

The estimates can be combined to give an upper bound for the degree need to approximate the function of interest $f(x; M_1, M_2)$ (Eq. 21) to a given accuracy.

Proposition 5.5. *Let $M_1, M_2 > 0$ and $\epsilon > 0$ be given and let*

$$R_1 = \lfloor r(eM_1/4, 5\epsilon/12) \rfloor \quad \text{and} \quad R_2 = \left\lfloor \frac{1}{2} r(eM_2/2, 5\epsilon/8) \right\rfloor.$$

Then

$$|E_{R_1}(x; M_1) C_{R_2}(x; M_2) - e^{-M_1 x^2} \cos(M_2 x)| \leq \epsilon,$$

$$|E_{R_2}(x; M_1) S_{R_2}(x; M_2) - e^{-M_1 x^2} \sin(M_2 x)| \leq \epsilon$$

for all $x \in [-1, 1]$.

Proof. With the above definitions of R_1, R_2 it follows from Lemma 5.2 and Lemma 5.4 that

$$|C_{R_2}(x; M_2) - \cos(M_2 x)| \leq \epsilon/2,$$
$$|S_{R_2}(x; M_2) - \sin(M_2 x)| \leq \epsilon/2,$$
$$|E_{R_1}(x; M_1) - e^{-M_1 x^2}| \leq \epsilon/2$$

for all $x \in [-1, 1]$. The statements now follow from the basic fact that if $||f - p||, ||g - q|| < \epsilon/2$ and $||g||, ||p|| \leq 1$, then

$$||fg - pq|| \leq ||f - p|| \cdot ||g|| + ||p|| \cdot ||g - q|| < \epsilon/2 + \epsilon/2 = \epsilon.$$

$\square$

To get a more explicit handle on the above estimate, we recall the following result of [GSLW19, lemma 59].

Lemma 5.6. *For $t \in \mathbb{R}_+$ and $\epsilon \in (0, 1)$ the following holds true*

$$et \geq \ln(1/\epsilon) \quad \Rightarrow \quad r(t, \epsilon) \leq et \tag{26}$$

$$et < \ln(1/\epsilon) \quad \Rightarrow \quad r(t, \epsilon) \leq \frac{\ln(1/\epsilon)}{\ln(e + \ln(1/\epsilon)/t)}.$$

Moreover, $r(t, \epsilon) = \Theta \left(t + \frac{\ln(1/\epsilon)}{\ln(e + \ln(1/\epsilon)/t)} \right)$.

6 End-to-end complexity

Given $T, \epsilon > 0$ and u_0, we will express the gate complexity of the version of the quantum algorithm needed to produce an estimate w_T of the exact solution u_T of the advection-diffusion equation with precision $\epsilon > 0$. In this endeavor we will make some simplifying assumptions. First, assume that

$$u_0(x) = \sum_{k=-N_0/2}^{N_0/2-1} \hat{u}(k) e_k(x), \tag{27}$$

for some even N_0. It is well-known that a sufficiently regular u_0 can be approximated uniformly by a finite Fourier series as above. In fact, estimating the coefficients via the discrete Fourier transform leads to a good uniform approximation for appropriately chosen N_0 (see, e.g., [Eps05] for detailed results in this direction).

The following lemma shows that an error made in representing the initial function propagates at worst linearly.

Lemma 6.1. *Let $u_t(x) = u(t, x)$ be a solution of $\partial_t u + c\partial_x u_x = \nu \partial_x^2 u$ in the domain $[0, d]$ with periodic boundary conditions. Then*

$$||u_t||_{L^2} \leq e^{-t\nu\omega^2}||u_0||_{L^2} + (1 + e^{-t\nu\omega^2})|\rho|, \tag{28}$$

where $\rho = d^{-1} \int_0^d u_0(x)dx$. In particular, $||u_t||_{L^2} \leq (1 + 2d^{-1/2})||u_0||_{L^2}$.

Proof. First, by introducing the change of variable $v(t,x) = u(t, x - ct)$, the equation $\partial_t u + c\partial_x u = \nu\partial_x^2 u$ is transformed into a pure heat equation $\partial_t v = \nu\partial_x^2 v$. With $\rho = d^{-1}\int_0^d u_0(x)dx$, we have the energy estimate (see for instance [QSS07, 13.1])

$$
\begin{aligned}
||u_t||_{L^2} = ||v_t||_{L^2} &\leq ||v_t - \rho||_{L^2} + |\rho| \leq e^{-t\nu\omega^2}||v_0 - \rho||_{L^2} + |\rho| \qquad (29)\\
&\leq e^{-t\nu\omega^2}||v_0||_{L^2} + (1 + e^{-t\nu\omega^2})|\rho| = e^{-t\nu\omega^2}||u_0||_{L^2} + (1 + e^{-t\nu\omega^2})|\rho|,
\end{aligned}
$$

proving the first estimate. For the final claim, note that $|c| \leq d^{-1}||u_0||_{L^1} \leq d^{-1/2}||u_0||_{L^2}$, which when combined with the first estimate yields $||u_t||_{L^2} \leq (1 + 2d^{-1/2})||u_0||$ as required. $\qquad\square$

As a consequence of the above, if u_t and u_t^* are solutions with different initial conditions, then $||u_t - u_t^*||_{L^2} \leq (1 + 2d^{-1})||u_0 - u_0^*||_{L^2}$, showing that the error at time t is controlled by the initial error. The more refined estimate in Equation (28) shows that the error made in the first Fourier mode is essentially preserved, while the errors made in the remaining modes dissipate with time.

Assume that $u_0(x)$ takes the form given in (27) and let u_t denote the corresponding exact solution. The associated difference-differential equation $\partial_t v = Lv_t$ for $L = -cD_{2p} + \nu D_{2p}^2$ (or $L = -cD_{2p} + \nu D_{2p}^{(2)}$) is in fact well-defined for all $x \in [0, d]$, and admits an explicit solution v_t subject to the same initial condition $v_0 = u_0$. In Theorem 7.4 in the next section, we establish the following estimate

$$
||u_T - v_T||_{L^2} \leq Te^{-\nu T\mu_1}(\Delta x)^{2p}B(u_0, c, \nu, p), \qquad \text{where} \qquad (30)
$$
$$
B(u_0, c, \nu, p) = \left[c^2 C_p^2||u_0^{(2p+1)}||_{L^2}^2 + \nu^2 C_p'^2||u_0^{(2p+2)}||_{L^2}^2\right]^{1/2},
$$

where C_p, C_p' are certain constants depending on p defined in the statement of the theorem and $\mu_1 = \mu_1(p, \Delta x)$ is an approximation of ω^2 defined in Equation (38). We would like to use this estimate to pin down the value of Δx, and hence n, to achieve a given accuracy ϵ. For that to work we need to remove the dependence of μ_1 on Δx. To this end, replace μ_1 by $\mu' = \mu_1(p, (\Delta x)_0)$ where N_0 is specified along with the initial function u_0 as in (27). Then for $\tau(T, \nu, p) := Te^{-\nu T\mu'}$ we have the bound

$$
||u_T - v_T||_{L^2} \leq \tau(T, \nu, p)(\Delta x)^{2p}B(u_0, c, \nu, p)
$$

for all $\Delta x \leq (\Delta x)_0$. To simplify the notation, we write $B = B(u_0, c, \nu, p)$ and $\tau = \tau(t, \nu, p)$. The quantum algorithm implements an approximation w_t to v_t that satisfies

$$
||w_t - v_t||_{L^2} \leq \epsilon'||u_0||_{L^2},
$$

where ϵ' is the precision in the polynomial approximation used in the QSVT algorithm.

To clarify the relationship between the various norms in use, we include the following simple result.

Lemma 6.2. *For an even positive integer N, let*

$$\mathcal{T}_N := \mathrm{Span}_{\mathbb{C}}\{e_k(x) = e^{i\omega k x} \colon -N/2 \le k < N/2\}.$$

equipped with the standard L^2 inner product on $[0, d]$. Then the evaluation map
$\mathrm{ev} \colon \mathcal{T}_N \to \mathbb{C}^N$ *given by* $\mathrm{ev}(q)_j = q(j\Delta x)$, $0 \le j < N$, *where $\Delta x = d/N$, is an isomorphism and*

$$||q||_{L^2} = (\Delta x)^{1/2}||\,\mathrm{ev}\, q||$$

where $\mathbb{C}^n$ is equipped with the standard Hermitian inner product.

Proof. The basic point is that the coefficients a_k specifying a given $q \in \mathcal{T}_N$ can be recovered by applying the (unitary) inverse Fourier transform (see Equation (13)) to $\mathrm{ev}(q)$ and scaling by $N^{-1/2}$. The norm comparison then follows from

$$d^{-1}||q||_{L^2} = \sum_k |a_k|^2 = N^{-1}||\,\mathrm{ev}(q)||.$$

$\square$

Theorem 6.3. *Assume that $u_0(x)$ is given by (27) and let $T > 0$ and $\epsilon > 0$ be given. Define*

$$n := \max\left\{ \left\lceil \log_2 \left(d\left(\frac{2\tau B}{\epsilon}\right)^{\frac{1}{2p}} \right) \right\rceil, \lceil \log_2 N_0 \rceil \right\},$$

and let $\Delta x = d/2^n$. Assume further that $q(x)$ is a polynomial satisfying

$$\sup_{x \in [-1,1]} |q(x) - e^{-M_1 x^2 + iM_2 x}| \le \frac{\epsilon}{2||u_0||_{L^2}},$$

where $M_1 = \frac{\nu T}{c_p^2 (\Delta x)^2}$, $M_2 = \frac{cT}{c_p \Delta x}$ and the constant c_p is given in (19). Then our quantum algorithm prepares a normalized approximation w_T/κ, $\kappa = ||u_0||_{L^2}(\Delta x)^{\frac{1}{2}}$, evaluated on the grid satisfying

$$||w_T - u_T||_{L^2} < \epsilon.$$

Proof. With the given choice of n, we obtain $\Delta x = d/2^n \le (\epsilon/(2\tau B))^{1/(2p)}$. By inserting this in the bound in Equation (30), we obtain $||u_T - v_T||_{L^2} \le \epsilon/2$. Next, let $H = i(\Delta x c_p)D_{2p}$ and $f(x) = e^{-M_1 x^2 + iM_2 x}$ with M_1 and M_2 specified as above. For a function $g \colon [0, d] \to \mathbb{R}$, let us write

$$\bar{g} = \mathrm{ev}(g) = \sum_{j=0}^{2^n - 1} g(j\Delta x)\,|j\rangle.$$

In this notation, we have $\bar{v}_T = f(H)\bar{u}_0$ and $\bar{w}_T = q(H)\bar{u}_0$. The spectral norm $||f(H) - p(H)||$ is plainly bounded above by $||f - q||_{\infty, [-1,1]}$. Hence,

$$||\bar{w}_T - \bar{v}_T|| = ||(q(H) - f(H))\bar{u}_0|| \le \frac{\epsilon||\bar{u}_0||}{2||u_0||_{L^2}}.$$

22

According to Lemma 6.2 this simplifies to $||w_T - v_T||_{L^2} \leq \epsilon/2$. We may now conclude that

$$||u_T - w_T||_{L^2} \leq ||u_T - v_T||_{L^2} + ||v_T - w_T||_{L^2} \leq \epsilon/2 + \epsilon/2 = \epsilon$$

as desired. $\qquad\square$

Using the explicit polynomial approximations laid out in the previous section, we obtain an estimate of the gate complexity of the quantum algorithm. The estimate depends on a somewhat technical assumption that stems from Lemma 5.6. After the proof we will explain why we consider this assumption to represent the generic case, and how to obtain the complexity if it fails to hold.

Theorem 6.4. *In the situation of Theorem 6.3, assume that*

$$n = \lceil \log_2(d(2\tau B \epsilon^{-1})^{1/(2p)}) \rceil \geq \lceil \log_2 N_0 \rceil \tag{31}$$

and that we use the polynomial approximation of Proposition 5.5. Then the gate complexity of the quantum circuit that prepares the approximate solution w_T/κ is

$$O\left(T \left(\frac{\nu(\tau B)^{\frac{1}{p}}}{c_p^2 \epsilon^{\frac{1}{p}}} + \frac{c(\tau B)^{\frac{1}{2p}}}{c_p \epsilon^{\frac{1}{2p}}} \right) \log_2 \left(d \left(\frac{\tau B}{\epsilon} \right)^{\frac{1}{2p}} \right) \log_2(p) \right), \quad \text{where} \tag{32}$$

$$B = \left[c^2 C_p^2 ||u_0^{(2p+1)}||_{L^2}^2 + \nu^2 C_p'^2 ||u_0^{(2p+2)}||_{L^2}^2 \right]^{1/2} \quad \text{and} \quad \tau = Te^{-\nu T \mu'}, \tag{33}$$

provided we make the following technical assumptions

$$\frac{e^2}{4} \frac{\nu T(\tau B)^{1/p}}{c_p^2 \epsilon^{1/p}} \geq \ln\left(\frac{48||u_0||_{L^2}}{5\sqrt{2}\epsilon} \right) \quad \text{and} \quad \frac{e^2}{2} \frac{cT(\tau B)^{1/(2p)}}{c_p \epsilon^{1/(2p)}} \geq \ln\left(\frac{32||u_0||_{L^2}}{5\sqrt{2}\epsilon} \right) \tag{34}$$

Proof. According to Lemma 4.9, the number of 1Q- and 2Q-gates used to apply the QSVT algorithm with the presented block encoding of D_{2p} and a polynomial q of degree $D + 1$ is $O(mnD)$, where $m = \lceil 2p + 1 \rceil$, and n, T and ϵ are given in the statement of the theorem. We clearly have $m = O(\log_2(p))$ and $n = O(\log_2(d(\tau B/\epsilon)^{1/(2p)}))$ due to Equation (31). It therefore suffices to show that D is bounded above by the first two factors in Equation (32) up to a constant.

By Proposition 5.5, if we set

$$q(x) = E_{R_1}(x; M_1)(C_{R_2}(x; M_2) + iS_{R_2}(x; M_2))$$

with R_1 and R_2 given by

$$R_1 = \left\lfloor r\left(\frac{eM_1}{4}, \frac{5\sqrt{2}\epsilon}{48||u_0||_{L^2}} \right) \right\rfloor \quad \text{and} \quad R_2 = \left\lfloor \frac{1}{2}r\left(\frac{eM_2}{2}, \frac{5\sqrt{2}\epsilon}{32||u_0||_{L^2}} \right) \right\rfloor, \tag{35}$$

then $|q(x) - e^{-M_1 x^2 + iM_2 x}| \leq \epsilon/(2||u_0||_{L^2})$ for all $x \in [-1, 1]$, thereby satisfying the requirement of Theorem 6.3. The corresponding degree is given by

$$D = 2(R_1 + R_2) \leq 2r(eM_1/4, 5\sqrt{2}\epsilon/(48||u_0||_{L^2})) + r(eM_1/2, 5\sqrt{2}\epsilon/(32||u_0||_{L^2})).$$

Recall that by Lemma 5.6, we have $r(M, \epsilon') < eM$ provided $eM > \ln(1/\epsilon')$. The technical assumptions ensure that this is valid in the two cases above. Indeed, from the formula for n in the statement of the theorem we obtain

$$\Delta x \leq (\epsilon/(\tau B))^{1/(2p)} \leq 2\Delta x \quad \Leftrightarrow \quad (\tau B/\epsilon)^{1/(2p)} \leq 1/\Delta x \leq 2(\tau B/\epsilon)^{1/(2p)}.$$

Hence, using that $M_1 = \nu T/(c_p \Delta x)^2$, we find

$$e\left(\frac{eM_1}{4}\right) = \frac{e^2}{4} \frac{\nu T (\tau B)^{1/p}}{c_p^2 \epsilon^{1/p}} \geq \ln\left(\frac{48||u_0||_{L^2}}{5\sqrt{2}\epsilon}\right),$$

which ensures that $r(eM_1/4, 5\sqrt{2}\epsilon/(48||u_0||_{L^2})) \leq \frac{e^2}{4} M_1$. A similar argument depending on the second technical assumption shows that $r(eM_2/2, 5\sqrt{2}\epsilon/(32||u_0||_{L^2}) \leq \frac{e^2}{2} M_2$. Consequently, $D \leq 2R_1 + R_2$ is bounded above by

$$\frac{e^2}{2}(M_1 + M_2) = \frac{e^2}{2}\left(\frac{\nu T}{c_p^2 \Delta x^2} + \frac{cT}{c_p \Delta x}\right) \leq e^2 T\left(\frac{2\nu(\tau B)^{1/p}}{c_p^2 \epsilon^{1/p}} + \frac{c(\tau B)^{1/(2p)}}{c_p \epsilon^{1/(2p)}}\right)$$

as required to establish the formula (32). $\qquad\square$

Let us now explain in what sense the technical assumptions (Eq. (34)) reasonably represent the generic case. First, let us remark that for all practical purposes we may take $p = O(1)$, since higher-order finite-difference approximations are unstable. With that in mind, we can take the various p-dependent constants c_p, C_p, C_p' to be $O(1)$. The technical assumptions can then be expressed in the form

$$\zeta T(\tau B)^s \geq \epsilon^s \ln(a/\epsilon) =: h(1/\epsilon),$$

where ζ is a constant absorbing c or ν, respectively, a is a constant and $s \in (0, 1)$. A simple exercise in calculus shows that $h(1/\epsilon) \leq h(1/(ae^{-1/s}) = a^s/(se)$. Moreover, it tends to zero as $\epsilon \to 0$. For a non-trivial problem, the left-hand-side is generally not artificially small and we therefore expect the inequalities to be valid.

Despite this heuristic, one can certainly choose the parameters so that the technical assumption fail. In that case, one obtains a different upper bound on D based on the second case given in Lemma 5.6, if $eM \leq \ln(1/\epsilon)$, then

$$r(M, \epsilon) \leq \frac{4\ln/1/\epsilon)}{\ln(e + \ln(1/\epsilon)/M)}.$$

We now establish the asymptotics of the constant c_p^{-1} encountered in the complexity statement.

Proposition 6.5. *The constant* $c_p^{-1} = \sum_{j=1}^p |\alpha_j|/j$, *where* $\alpha_j = 2(-1)^{j+1}\frac{(p!)^2}{(p+j)!(p-j)!}$ *satisfies* $c_p^{-1} = \Theta(\log p)$.

Proof. First, note that

$$|\alpha_j| = \frac{2(p!)^2}{(p+j)!(p-j)!} = 2\prod_{s=1}^{j}\frac{p+s-j}{p+s} = 2\prod_{s=1}^{j}\left(1-\frac{j}{p+s}\right).$$

Hence, $|\alpha_j| \leq 2$ for all j, so that $c_p^{-1} \leq 2\sum_{j=1}^{p}1/j = O(\log(p))$. To establish the lower bound, observe that for $j \leq \sqrt{p}-1$

$$\frac{1}{2}|\alpha_j| = \prod_{s=1}^{j}\left(1-\frac{j}{p+s}\right) \geq \left(1-\frac{j}{p}\right)^j \geq \left(1-\frac{\sqrt{p}}{p}\right)^{\sqrt{p}-1} \geq e^{-1}.$$

Hence, for $r = \lfloor\sqrt{p}\rfloor - 1$

$$c_p^{-1} \geq \sum_{j=1}^{r}|\alpha_j|/j \geq 2e^{-1}\sum_{j=1}^{r}1/j = \Omega(\log(r)) = \Omega(\log(p))$$

establishing the desired result. $\qquad\square$

To conclude, we include a simplified complexity statement in the $\widetilde{O}$ notation that ignores logarithmic factors.

Corollary 6.5.1. *Consider the situation of Theorem 6.3 and take the assumptions in Theorem 6.4 for granted. Then, in the pure advection case, $\nu = 0$, the complexity is given by*

$$\tilde{O}\left((cT)^{1+\frac{1}{2p}}||u_0^{(2p+1)}||_{L^2}^{\frac{1}{2p}}\log_2(p)^2\epsilon^{-\frac{1}{2p}}\right), \tag{36}$$

and in the pure diffusion case, $c = 0$, the complexity is given by

$$\tilde{O}\left((\nu T)^{1+\frac{1}{p}}e^{-\nu T\mu'/p}||u_0^{(2p+2)}||_{L^2}^{\frac{1}{p}}\log_2(p)^3\epsilon^{-\frac{1}{p}}\right). \tag{37}$$

Proof. If $\nu = 0$, then $B = cC_p||u_0^{(2p+1)}||_{L^2}$ and $\tau = T$. Moreover, $C_p = (p!)^2/(2p+1)! \leq (p!)^2/(2p)! \leq 2^{-p}$, so that $C_p^{1/(2p)} = O(1)$. Inserting these in formula (32), ignoring the logarithmic factor and using that $c_p^{-1} = \Theta(\log p)$ leads to the stated formula. The case $c = 0$ follows in the same manner. $\qquad\square$

Remark. *The formula (37) may seem to indicate that the complexity tends to zero as $T \to \infty$. However, assumption (31) will fail for sufficiently large T, making the complexity formula invalid.*

7 Numerical estimates

The purpose of this section is to establish the previously introduced error estimate (30). Recall that we work in the spatial domain $[0,d]$ with an even

number N of uniformly distributed grid points. Moreover, $e_k(x) = e^{i\omega kx}$ for $k \in \mathbb{Z}$, where $\omega = 2\pi/d$, and the finite difference operators δ_j, D_{2p} and $D_{2p}^{(2)}$ were introduced in equation (9) and theorem 2.1.

For any $k \in \mathbb{Z}$, we have $\partial_x e_k(x) = i\omega k e_k(x)$ and $\partial_x^2 e_k(x) = -\omega^2 k^2 e_k(x)$. Similarly, by inspection

$$\delta_{2j} e_k(x) = i\frac{\sin(\omega k j \Delta x)}{j\Delta x} e_k(x) \quad \text{and} \quad \delta_j^2 e_k(x) = -\frac{2 - 2\cos(\omega k j \Delta x)}{(j\Delta x)^2} e_k(x).$$

By linearity, one obtains $D_{2p} e_k(x) = i\lambda_k(x)$ and $D_{2p}^{(2)} e_k(x) = -\mu_k e_k(x)$, where

$$\lambda_k := \sum_{j=1}^{p} \alpha_j \frac{\sin(\omega k j \Delta x)}{j\Delta x} \quad \text{and} \quad \mu_k := \sum_{j=1}^{p} \alpha_j \frac{2 - 2\cos(\omega k j \Delta x)}{(j\Delta x)^2}. \tag{38}$$

We will now establish some facts about the quality of the approximations $\lambda_k \approx \omega k$ and $\mu_k \approx \omega^2 k^2$.

Lemma 7.1. *Let p be a positive integer and let $\alpha_j = 2(-1)^{j+1}\frac{(p!)^2}{(p+j)!(p-j)!}$ for $1 \leq j \leq p$. Then for $h \in \mathbb{R}$ the following identity holds true*

$$\sum_{j=1}^{p} \alpha_j \cos(jh) = 1 - 2^{2p} \binom{2p}{p}^{-1} \sin(h/2)^{2p}.$$

Proof. We compute using the binomial formula

$$(2i\sin(h/2))^{2p} = (e^{ih/2} - e^{-ih/2})^{2p} = \sum_{j=0}^{2p} \binom{2p}{j}(-1)^j e^{i(j-p)h}$$

$$= (-1)^p \left[\binom{2p}{p} + \sum_{j=1}^{p} \binom{2p}{p-j}(-1)^j e^{-ijh} + \sum_{j=1}^{p} \binom{2p}{p+j}(-1)^j e^{ijh} \right]$$

$$= (-1)^p \left[\binom{2p}{p} + \sum_{j=1}^{p} 2(-1)^j \binom{2p}{p+j} \cos(jh) \right].$$

In the passage to the second line, the sum is first split into three parts $0 \leq j \leq p - 1$, $j = p$ and $p + 1 \leq j \leq 2p$, followed by the change of variables $j \mapsto p - j$ in the first sum and $j \mapsto j + p$ in the third sum. The desired formula is obtained by multiplying by $(-1)^p \binom{2p}{p}^{-1}$, rearranging and using the fact that $\alpha_j = (-1)^{j+1} \binom{2p}{p+j} \binom{2p}{p}^{-1}$. $\square$

Theorem 7.2. *For a fixed positive integer p, let $\lambda(k) := \lambda_k$ and $\mu(k) := \mu_k$ be defined by the formulas in (38). Then the following hold true.*

(a) $\lambda(-k) = -\lambda(k)$ and $\mu(-k) = \mu(k)$.

(b) $\lambda(k) \leq \omega k$ and $\mu(k) \leq \omega^2 k^2$ for all $k \geq 0$.

(c) The function $k \mapsto \mu(k)$ is increasing on $\in [0, N/2]$ and decreasing on $[-N/2, 0]$. The function $\lambda(k)$ is positive on $[0, N/2]$ and negative on $[-N/2, 0]$.

(d) We have the following estimates

$$|\omega k - \lambda_k| \leq \frac{(p!)^2}{(2p+1)!} |\omega k|^{2p+1} (\Delta x)^{2p}$$

$$|\omega^2 k^2 - \lambda_k^2| \leq \frac{2(p!)^2}{(2p+1)!} |\omega k|^{2p+2} (\Delta x)^{2p}$$

$$|\omega^2 k^2 - \mu_k| \leq \frac{2(p!)^2}{(2p+2)!} |\omega k|^{2p+2} (\Delta x)^{2p}.$$

Proof. Part (a) is evident from the formulas in (38). For part (b), observe first that by Lemma 7.1

$$\lambda'(k) = \omega \sum_{j=1}^{p} \alpha_j \cos(\omega k j \Delta x) = \omega \left(1 - C \sin(\omega k \Delta x/2)^{2p}\right), \qquad (39)$$

where $C := 2^{2p} \binom{2p}{p}^{-1}$. Set $f(k) = \omega k - \lambda(k)$. As $f(0) = 0$ and

$$f'(k) = \omega - \lambda'(k) = \omega C \sin(\omega k \Delta x/2)^{2p} \geq 0 \quad \text{for all } k \in \mathbb{R},$$

it follows that $f(k) \geq 0 \Leftrightarrow \lambda(k) \leq \omega k$ for $k \geq 0$, proving the first part of (b). Next, notice that

$$\mu'(k) = 2\omega \sum_{j=1}^{p} \alpha_j \frac{\sin(\omega k j \Delta x)}{j \Delta x} = 2\omega \lambda(k).$$

Hence, for $g(k) := \omega^2 k^2 - \mu(k)$ we obtain $g'(k) = 2\omega(\omega k - \lambda_k) \geq 0$ for $k \geq 0$. As $g(0) = 0$, it follows that $g(k) \geq 0$ or equivalently $\mu(k) \leq \omega^2 k^2$ for all $k \geq 0$. This proves the second part of (b).

For part (c) it suffices to show that $\mu'(k) = 2\omega \lambda(k) \geq 0$ for $k \in [0, N/2]$. Using equation (39) we find

$$\lambda''(k) = -(pC\omega^2 \Delta x) \cos(\omega k \Delta x/2) \sin(\omega k \Delta x/2)^{2p-1}.$$

Now, $k \in [0, N/2]$ if and only if $\omega k \Delta x/2 = \pi k/N \in [0, \pi/2]$, from which we can conclude that $\lambda''(k) \leq 0$ for $k \in [0, N/2]$, that is, λ is concave. By inspection, $\lambda(0) = \lambda(N/2) = 0$, so by Jensen's inequality it follows that $\lambda(k) \geq 0$ for $k \in [0, N/2]$.

For part (d), we assume without loss of generality that $k \geq 0$ and estimate

$$\omega k - \lambda_k = f(k) - f(0) = \int_0^k f'(s) ds = \omega C \int_0^k \sin(\omega s \Delta x/2)^{2p} ds$$

$$\leq \omega C \int_0^k (\omega s \Delta x/2)^{2p} ds = \frac{(p!)^2}{(2p+1)!} (\omega k)^{2p+1} (\Delta x)^{2p},$$

where we have used that $C = 2^{2p}\binom{2p}{p}^{-1}$. Next, by part (b)

$$|\omega^2 k^2 - \lambda_k^2| = |\omega k + \lambda_k||\omega k - \lambda_k| \le 2\omega|k||\omega k - \lambda_k|.$$

The second formula follows by combining this with the first estimate. The final estimate can be deduced from the first one as follows

$$\omega^2 k^2 - \mu_k = g(k) - g(0) = \int_0^k g'(s)ds = 2\omega \int_0^k \omega s - \lambda(s)ds$$

$$\le 2\omega \frac{(p!)^2}{(2p+1)!}\omega^{2p+1}(\Delta x)^{2p}\int_0^k s^{2p+1}ds = \frac{2(p!)^2}{(p+2)!}(\omega k)^{2p+2}(\Delta x)^2$$

$\square$

We need an additional lemma to establish the desired error estimate.

Lemma 7.3. *For* $z, w \in \mathbb{C}$ *it holds true that*

$$|e^z - e^w| \le e^{\max(\operatorname{Re} z, \operatorname{Re} w)}|z - w|.$$

Proof. Parametrize the line segment L from w to z by $\gamma(t) = w + t(z - w)$, $t \in [0, 1]$. Set $b = \operatorname{Re} z$ and $a = \operatorname{Re} w$. We compute

$$|e^z - e^w| = \left|\int_L e^u du\right| = \left|\int_0^1 e^{w+t(z-w)}(z - w)dt\right|$$

$$\le \int_0^1 e^{a+t(b-a)}dt|z - w| = \frac{e^b - e^a}{b - a}|z - w| \le e^{\max(a,b)}|z - w|,$$

where the final inequality follows from the mean value theorem. $\square$

The following theorem contains the desired error estimate. In order to obtain a precise result, we assume that the initial function is exactly representable with N Fourier modes, that is, $u_0(x) = \sum_{-N/2 \le k < N/2} a_k e_k(x)$.

Theorem 7.4. *Fix a positive integer* p. *Let*

$$u(t, x) = \sum_{k=-N/2}^{N/2-1} a_k e^{-ic\omega kt - \nu\omega^2 k^2 t} e_k(x)$$

$$v(t, x) = \sum_{k=-N/2}^{N/2-1} a_k e^{-ic\lambda_k t - \nu\mu_k t} e_k(x),$$

where λ_k *and* μ_k *are given in* (38)*, be the solutions of the equations*

$$\partial_t u(t, x) = (-c\partial_x + \nu\partial_x^2)u(t, x) \quad and \quad \partial_t v(t, x) = (-cD_{2p} + \nu D_{2p}^{(2)})v(t, x),$$

respectively, with the same initial condition. Then

$$||u_t - v_t||_{L^2} \le te^{-\nu t\mu_1}(\Delta x)^{2p}\left[c^2 C_p^2||u_0^{2p+1}||_{L^2}^2 + \nu^2(C_p')^2||u_0^{(2p+2)}||_{L^2}^2\right]^{1/2}, \quad (40)$$

where $u_t(x) = u(t, x)$, $v_t(x) = v(t, x)$, $C_p = \frac{(p!)^2}{(2p+1)!}$ *and* $C_p' = \frac{2(p!)^2}{(2p+2)!}$.

Proof. Without loss of generality, we work with the normalized L^2 norm for which $||e_k(x)||_{L^2} = 1$ for all k. Throughout the proof, all sums are taken from $-N/2$ to $N/2 - 1$. Set $z_k = -ic\omega kt - \nu\omega^2 k^2 t$ and $w_k = -ic\lambda_k t - \nu\mu_k t$. By Lemma 7.3,

$$||u_t - v_t||_{L^2}^2 = \sum_k |a_k|^2 |e^{z_k} - e^{w_k}|^2 \leq \sum_k |a_k|^2 e^{2\max(\operatorname{Re} z_k, \operatorname{Re} w_k)} |z_k - w_k|^2. \quad (41)$$

By Theorem 7.2, $\max(\operatorname{Re} z_k, \operatorname{Re} w_k) = -\nu t\mu_k$ and

$$\begin{aligned}
|z_k - w_k|^2 &= (ct)^2 |\omega k - \lambda_k|^2 + (\nu t)^2 |\omega^2 k^2 - \mu_k|^2 \\
&\leq (t(\Delta x)^{2p})^2 ((cC_p|\omega k|^{2p+1})^2 + (\nu C_p'|\omega k|^{2p+2})^2),
\end{aligned} \quad (42)$$

for all $|k| \leq N/2$. The desired estimate is obtained by combining this with (41) as follows

$$\begin{aligned}
||u_t - v_t||_{L^2}^2 &\leq (t(\Delta x)^{2p})^2 \sum_k |a_k|^2 e^{-2\nu t\mu_k} \left((cC_p|\omega k|^{2p+1})^2 + (\nu C_p'|\omega k|^{2p+2})^2 \right) \\
&\leq (te^{-\nu t\mu_1}(\Delta x)^{2p})^2 \sum_k |a_k|^2 \left((cC_p|\omega k|^{2p+1})^2 + (\nu C_p'|\omega k|^{2p+2})^2 \right) \\
&= (te^{-\nu t\mu_1}(\Delta x)^{2p})^2 \left(c^2 C_p^2 ||u_0^{2p+1}||_{L^2}^2 + \nu^2 (C_p')^2 ||u_0^{(2p+2)}||_{L^2}^2 \right).
\end{aligned}$$

Here we have used $\mu_1 \leq \mu_k$ for all $0 < |k| \leq N/2$ by Theorem 7.2, and the fact from Fourier analysis that $||u_0^{(m)}||_2^2 = \sum_{k \in \mathbb{Z}} |\omega k|^m |a_k|^2$ for $m \geq 0$. $\qquad\square$

Remark. *The same result is true with $D_{2p}^{(2)}$ replaced by D_{2p}^2, provided we make the following modifications.*

- *Replace μ_k by λ_k^2 in the definition of $v(t,x)$, and μ_1 by λ_1^2 in the main estimate.*

- *Replace the constant C_p' in the main estimate by $C_p'' = \frac{2(p!)^2}{(2p+1)!}$ (compare the estimates in theorem 7.2 part (d)).*

8 The higher-dimensional case

Consider the general advection-diffusion equation

$$\partial_t u + c \cdot \nabla u = \nu \Delta u,$$

where $\nabla u = (\partial_{x_1} u, \partial_{x_2} u, \ldots, \partial_{x_n} u)$ is the gradient and $\Delta u = \sum_{j=1}^n \partial_{x_j}^2 u$ is the Laplacian. Then

$$P = -c \cdot \nabla + \nu\Delta = \sum_{j=1}^n -c_j \partial_{x_j} + \nu \partial_{x_j}^2 =: \sum_{j=1}^n P_j.$$

If we use a multi-dimensional uniform grid with N points in each coordinate direction, the underlying discrete space is

$$\mathbb{R}^{N^d} = (\mathbb{R}^N)^{\otimes d} \cong \mathbb{R}^N \otimes \mathbb{R}^N \otimes \cdots \otimes \mathbb{R}^N.$$

If we use our 1-dimensional finite-difference approximations $P_j \approx L_j$ in each coordinate direction, we obtain the finite-difference approximation $L \approx P$ given in terms of the above tensor decomposition by

$$L = \sum_{j=1}^{n} I^{\otimes(j-1)} \otimes L_j \otimes I^{\otimes(n-j)}.$$

The associated difference-differential equation becomes $V'(t) = LV(t)$, with solution

$$V(t) = e^{Lt}V_0 = \left(\bigotimes_{j=1}^{n} e^{tL_j} \right) V_0. \tag{43}$$

This n-dimensional approximation can therefore be implemented by composing the 1-dimensional approximations using Lemma 3.2. For example, for $d = 2$,

$$e^{Lt} = (e^{L_1 t} \otimes I) \circ (I \otimes e^{L_2 t}). \tag{44}$$

However, we do not advocate this approach in general for $d \leq 2$. First, there are more efficient finite-difference stencils than the ones obtained with this strategy, and second applying the composition Lemma multiple times will quickly become problematic in the post-selection stage.

9 Numerical results

In this section, we display numerical results with a computational implementation of the quantum algorithm for finite-difference operators of orders $2p = 2, 4, 6, 14$ proposed in this paper for a selection of initial conditions, times, and parameters. The code is written in qiskit [JATK+24] and is available in an accompanying Github repository [HO25]. The quantum circuits are simulated with the freely available aer simulator. For the purpose of displaying the internal accuracy of the algorithm, we have used exact statevector simulation, and compared the results to a high accuracy Fourier approximation (error $\sim 10^{-8}$ using the error formula below (45)) of the exact solution given in Equation 8. In the case of pure advection, the exact solution $u(t, x - ct)$ is used instead. The error displayed is computed as

$$\text{error} = \max_{0 \leq j < 2^n} ||v_T(j\Delta x) - u_T(j\Delta x)||, \tag{45}$$

where v_T is the solution computed by the quantum algorithm after rescaling and u_T is the (approximate) exact solution. Note that the cost of preparing the

initial state, a normalized version of $u_0(x)$ evaluated on the grid, is not included in the reported gate counts.

We are particularly interested in comparing the numerical behaviour at different orders, where a finer resolution, that is, additional spatial qubits, are used at lower order to achieve a similar accuracy to the simulation at higher order. We use the spatial domain $[0, 4]$ throughout. Therefore, n spatial qubits correspond to 2^n grid points and a step size of $\Delta x = 2^{2-n}$. The resources used in the runs are quantified in terms of gate counts; CNOT-gates and 1-qubit gates, the total number of qubits and the accuracy of the output.

Since our algorithm depends on block encoding, one has to post-select on the ancilla register being in the $|0\rangle$-state. The one-dimensional version introduces the scaling factor $\frac{1}{2}$ due to our use of Corollary 3.1.1. In addition, we introduce a scaling factor 0.95 when computing the angle sequence associated with the Chebyshev coefficients for numerical stability. This leads to a reduced success probability of $(0.95 \times 0.5)^2 \approx 0.2256$. For pure advection, the simulated evolution is approximately unitary, so we expect to be close to this success rate. When diffusion is present, the L^2 norm of the solution will decrease with time towards a lower bound and this is necessarily reflected in the success probabilities. In the two-dimensional case, the scaling factor is squared $(0.95 \times 0.5)^4 \approx 0.0509$, since we compose two instances of the one-dimensional algorithm (see (44)) using the composition Lemma 3.2.

9.1   1D tests

Gaussian wave   In a first test, we consider the case of pure advection ($\nu = 0$) with speed $c = 1$ and Gaussian initial data $u_0(x) = e^{-10(x-5/3)^2}$ that is run until time $T = 4$, corresponding to a full period (Figure 3 and Table 1).

We compare the order 2 method with 8 and 9 spatial qubits, respectively, to the order 6 method with 6 and 7 spatial qubits, respectively (bottom panel in Figure 3). The numerical results are visually indistinguishable from the exact solution, and this is reflected in the error values displayed in Table 1. The order 6 method outperforms the order 2 method on all parameters: accuracy, gate counts and total qubit count. Indeed, both the run at order 2 with 9 spatial qubits and the run at order 6 with 6 spatial qubits have an error $\sim 10^{-3}$, but the order 2 method uses ~ 2.5 times as many CNOT and 1-qubit gates.

It is also interesting to see how the gate count and accuracy scale as the number of spatial qubits is increased by one. Note that this corresponds to replacing the step size Δx by $\Delta x/2$. For the order 2 method, the accuracy improves by around a factor of ten, while the gate count roughly doubles. For the order 6 method the accuracy improves by a factor of 10^{-2}, while the gate count scales slightly better than in the second order method.
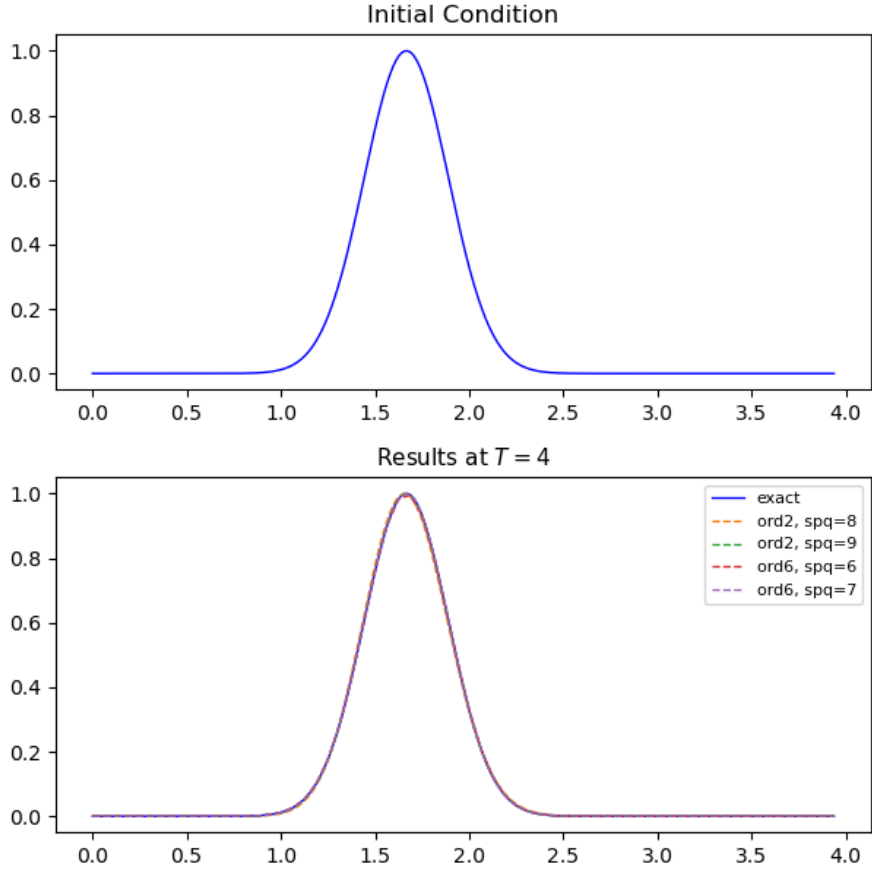
31

Figure 3: Comparison of methods of order 2 and 6 and exact solution (bottom panel) for the QSVT-based solution of the 1D advection equation with speed $c = 1$ and Gaussian initial conditions $u_0(x) = \exp(-10(x - 5/3)^2)$ (top panel). The number of spatial qubits used is denoted by spq.

Order	Spatial qubits	Total qubits	Error (sv)	Success rate	1-qubit gates	CNOT gates
2	8	12	2.042e-02	0.2256	23433	16150
2	9	13	5.047e-03	0.2256	49298	33889
6	6	11	1.856e-03	0.2256	18658	13636
6	7	12	3.298e-05	0.2256	37386	27130

Table 1: Data table for the 1D Gaussian wave simulation in Figure 3.

Sum of sine waves Next, we consider the pure diffusion equation ($c = 0$) with $\nu = 0.02$, and initial data

$$u_0(x) = 1 + \frac{1}{2}\sin\left(\frac{3\pi}{2}x\right) + \frac{1}{2}\sin\left(\frac{11\pi}{2}x\right) \tag{46}$$
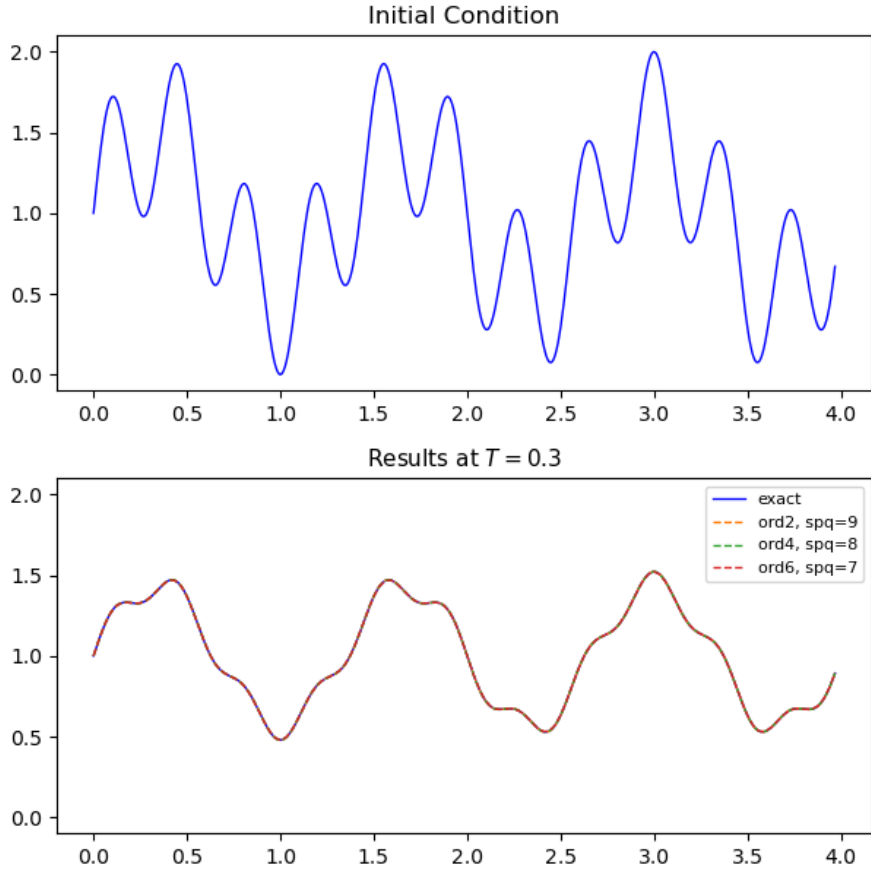
evolved until time $T = 0.3$ (Figure 4 and Table 2).

Figure 4: Comparison of QSVT-based methods of order 2, 4 and 6 and exact solution (bottom panel) for the pure diffusion equation with $\nu = 0.2$ and initial condition a sum of sine waves (top panel, Eq. (46)). The number of spatial qubits used is denoted by spq.

33

Order	Spatial qubits	Total qubits	Error (sv)	Success rate	1-qubit gates	CNOT gates
2	9	12	9.362e-04	0.7937	10884	7686
4	8	12	5.256e-05	0.7937	10069	7459
6	7	11	4.998e-05	0.7937	5378	3054

Table 2: Data table for the sum of sine waves simulation in Figure 4.

Here, we compare the methods of order 2, 4 and 6, with 9, 8 and 7 spatial qubits, respectively. The error is $\sim 10^{-5}$ in each case, and the numerical solutions are visually indistinguishable from the exact solution in Figure 4. The methods of order 2 and 4 have almost identical total qubit counts and gate counts. In contrast, the order 6 method uses one qubit less and about ~ 0.5 the number of gates. The fact that the step from order 4 to 6 reduces the gate count drastically, while the step from order 4 to 2 does not, can be explained as follows. The methods of order 4 and 6 utilize 4 ancilla qubits (the difference between the total number and the number of spatial qubits in Table 2), while the order 2 method needs 3 ancilla qubits. In fact, the order 6 method is the highest order method we can realize with 3 ancilla qubits using our approach. In other words, the order 4 method is utilizing the ancilla qubits less effectively than the order 6 method, and this is reflected in the gate counts.

Wave packet   Next, we consider a wave packet given by

$$u_0(x) = \frac{3}{5} + \frac{1}{2}e^{-5(x-2)^2}\cos\left(\frac{17\pi}{2}(x-2)\right) \tag{47}$$

subject to advection with $c = 1$ and mild diffusion with $\nu = 10^{-3}$, evolved until time $T = 1.5$ (Figure 5 and Table 3).

Here we compare the order 6 method with 8 and 9 spatial qubits, respectively, to the order 14 method with 6 and 7 qubits, respectively. In contrast to the previous runs, the order 6 method outperforms the order 14 method in accuracy. With 8 spatial qubits for the order 6 method and 6 spatial qubits for the order 14 method, the gate counts are slightly in favor of the higher order method, but its accuracy is worse by two orders of magnitude. With one additional spatial qubit for both methods, the lower order method still has superior accuracy, albeit with a narrower gap. The poor performance of the order 14 method can be explained by the fact that the initial function needs more than 6 spatial qubits to be properly resolved. It is only when the mesh resolves the Fourier modes present in the initial function that the higher order methods truly dominate in performance.
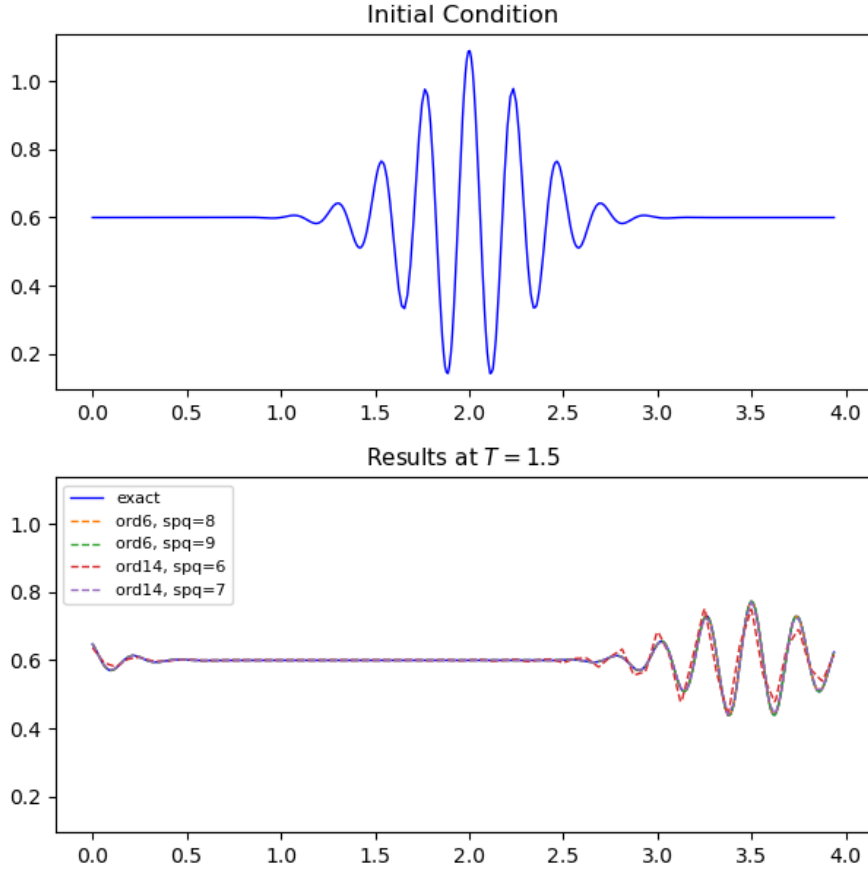
34

Figure 5: Comparison of QSVT-based methods of order 6 and 14 and exact solution (bottom panel) for the advection-diffusion equation with $c = 1$, $\nu = 10^{-3}$ and initial data a wave packet (top panel, Equation (47))

Order	Spatial qubits	Total qubits	Error (sv)	Success rate	1-qubit gates	CNOT gates
6	8	13	2.662e-04	0.2398	27135	19578
6	9	14	4.334e-06	0.2398	55333	39729
14	6	12	5.429e-02	0.2399	21663	17331
14	7	13	1.483e-05	0.2398	40290	32029

Table 3: Data table for the wave pack simulation in Figure 5.

The rectangle function   Here we consider a non-smooth rectangle function given by

$$u_0(x) = \begin{cases} 1 & \text{if } 0 \leq x \leq 2 \\ 0 & \text{if } 2 < x < 4 \end{cases} \tag{48}$$

subject to advection with $c = 1$ and diffusion with $\nu = 0.02$ for an evolution time of $T = 1$ (Figure 6 and Table 4).

We compare the methods of order 2 and 6 with 8 and 7 spatial qubits, respectively. Both runs achieve an error of order $\sim 10^{-2}$ with the same total number of qubits. The order 2 method is superior in terms of gates and is therefore favored over the order 6 method in this case. Since higher order methods are only effective when the initial data is correspondingly regular, these results are not surprising.

We regard this example as an application of our algorithm to state preparation. The rectangle function is easily prepared with Hadamard gates on the first half of the spatial qubits. By evolving this function with the second order method, we prepare an approximate bump function. The center and slope of the bump function can be controlled through the advection and diffusion parameters, respectively.

Order	Spatial qubits	Total qubits	Error	Success rate	1-qubit gates	CNOT gates
2	8	12	3.323e-02	0.2218	8607	5970
6	7	12	3.376e-02	0.2219	13187	9569

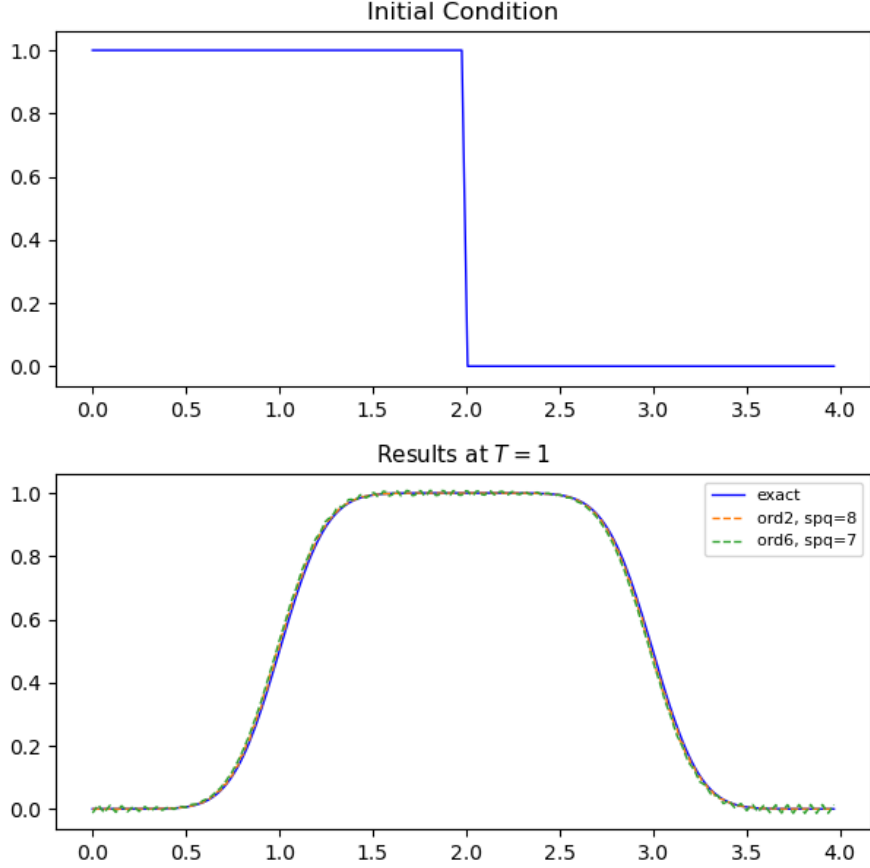Table 4: Data table for the rectangle function simulations in Figure 6.

Figure 6: Comparison of QSVT-based methods of order 2 and 6 and exact solution (bottom panel) for the advection-diffusion equation with $c = 1$, $\nu = 0.2$ and initial data a rectangle function (top panel, Eq. (48)).

9.2 2D tests

Two-dimensional Gaussian Here we consider pure advection with velocity $c = (3/2, 2/3)$ and initial data

$$u_0(x, y) = \exp(-7(x - 5/3)^2 - 7(y - 2)^2) \tag{49}$$

evolved until time $T = 0.8$ (Figure 7 and Table 5).

We compare the order 2 method with 14 spatial qubits (7 in each coordinate direction) to the order 6 method with 12 spatial qubits. In this 2-dimensional case, the superiority of the higher order method is even more evident than in the 1D cases. With about 2/3 of the gate count and similar qubit usage, the order 6 methods achieves an accuracy of two orders of magnitude better

37

than the order 2 method. This is expected from the one-dimensional results, since the two-dimensional algorithm is constructed from two instances of the 1-dimensional algorithm. The success rate is significantly lower than in the $1d$ case, which is a consequence of the construction. The success probability will roughly correspond to the square of the probability for the corresponding one-dimensional problem.
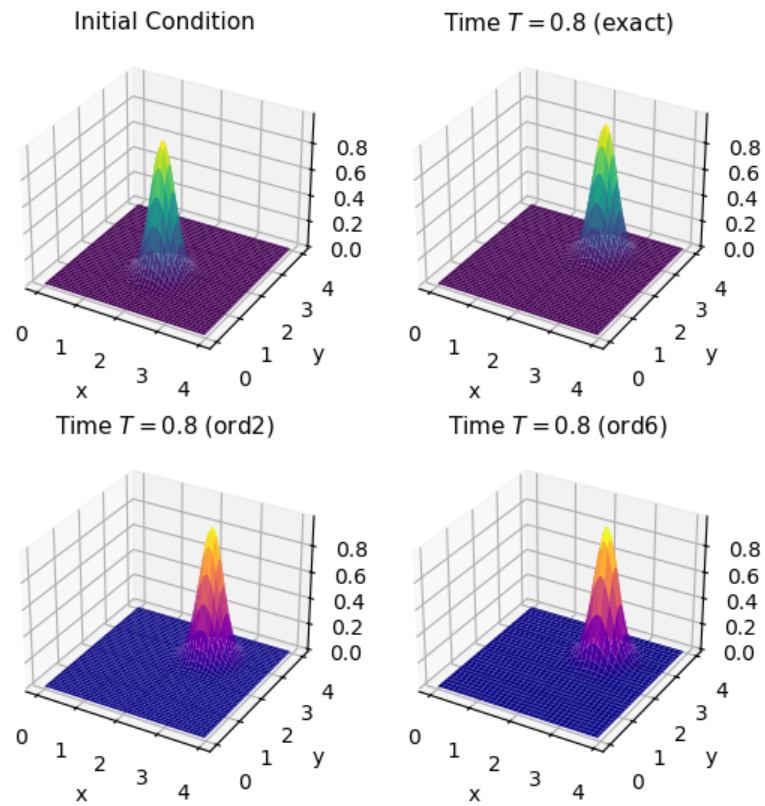

Figure 7: Comparison of QSVT-based methods of order 2 and 6 (bottom panels) and exact solution (top right panel) for the 2D advection equation with $c = (3/2, 2/3)$ and Gaussian initial data (top left panel, Eq. (49)).

Order	Spatial qubits	Total qubits	Error	Success rate	1-qubit gates	CNOT gates
2	14	19	1.678e-02	0.0509	24468	21953
6	12	18	2.164e-04	0.0509	17054	13269

Table 5: Data table for the two-dimensional Gaussian simulation in Figure 7.

A mixed wave We consider mixed advection-diffusion with $c = (1, 0.5)$, $\nu = 0.2$ and the slightly more exotic initial function

$$u_0(x, y) = e^{-7(x-2)^2}(1 + \sin(5\pi y/2)), \tag{50}$$

evolved until time $T = 0.4$ (Figure 8 and Table 6).

We compare the methods of order 2 and 6 with 16 and 14 spatial qubits, respectively. The order 6 method is far superior. With fewer qubits and about one third of the gate count, the sixth-order method achieves an accuracy of $\sim 10^{-6}$, which is three orders of magnitude better than the second order method.

Order	Spatial qubits	Total qubits	Error	Success rate	1-qubit gates	CNOT gates
2	16	21	2.929e-03	0.0478	73580	71047
6	14	20	1.858e-06	0.0477	28776	25127

Table 6: Data table for the mixed wave simulation in Figure 8.

10 Conclusions and future work

This paper introduced a quantum algorithm based on the quantum singular value transform for the simulation of the linear advection-diffusion equation. In order to apply the QSVT algorithm, we laid out a general framework for constructing block-encodings of finite-difference operators and worked out the construction in detail for symmetric operators of arbitrary order in one dimension.

The main contributions of this work are the construction and complexity analysis for the concrete problem of advection-diffusion simulation, and an accompanying end-to-end implementation of a number of specific instances of the proposed algorithm. Moreover, our numerical simulations of the algorithm showed that it can be used with $\sim 10 - 12$ logical qubits and a few thousands of $CNOT$ and 1-qubit gates depending on the tunable parameters. The theoretical complexity statement and the numerical simulations showed a high order of compatibility and demonstrated clearly the superior performance of the higher order methods, with some minor caveats.
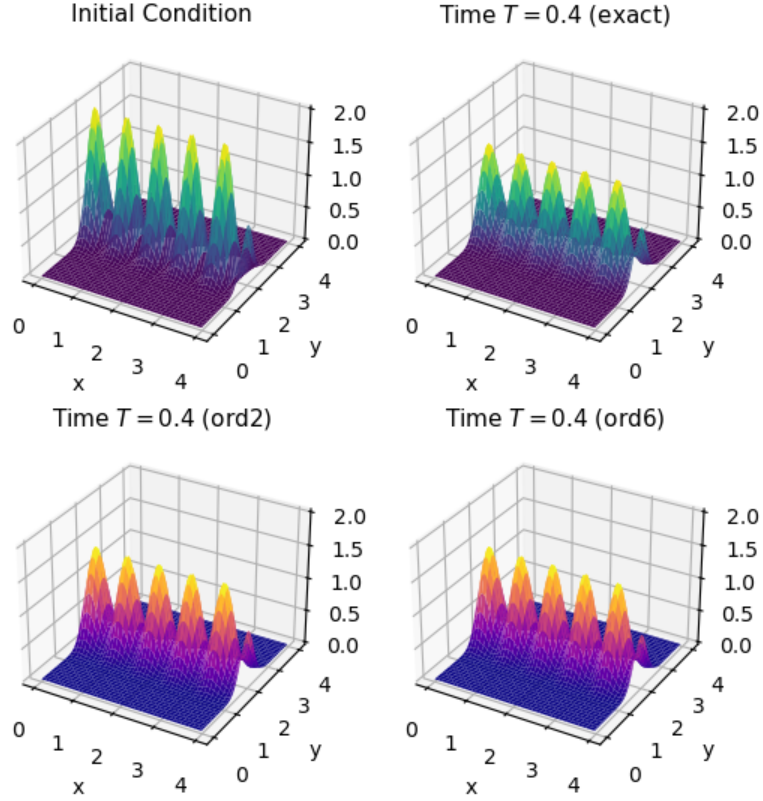
Figure 8: Comparison of QSVT-based methods of order 2 and 6 (bottom panels) and exact solution (top right panel) for the 2D advection-diffusion equation with $c = (1, 0.5)$, $\nu = 0.2$ and initial data a mixed wave (top left panel, Eq. (50)).

The results of this paper lay the groundwork for a number of extensions towards quantum simulation of more complex fluid flow models. First, the extension to higher dimensional linear advection-diffusion can be done more efficiently than the basic method used in this paper. More general linear equations can also be considered. These topics have been investigated in the quantum computing literature, but there is typically still a rather large gap between the high-level algorithms constructed and efficient implementation in practice. Of greater interest is the extension to non-linear models such as Burgers' equation, the shallow water equations and eventually the compressible Navier-Stokes equations. Here, the shallow water equations is a natural intermediate test case.

Finally, comparison with classical algorithms will be extended to ascertain the efficiency potential of quantum algorithms in full-fledged models, with a specific outlook to operational requirements in numerical weather prediction.

References

[AA22]   Amol Aggarwal and Josh Alman. Optimal-degree polynomial approximations for exponentials and gaussian kernel density estimation, 2022.

[Aar04]   Scott Aaronson. Quantum computing, postselection, and probabilistic polynomial-time. *Proceedings of the Royal Society A: Mathematical, Physical and Engineering Sciences*, 461:3473 – 3482, 2004.

[ACL23]   Dong An, Andrew M. Childs, and Lin Lin. Quantum algorithm for linear non-unitary dynamics with near-optimal dependence on all parameters. *arXiv e-prints*, page arXiv:2312.03916, December 2023.

[AS64]   Milton Abramowitz and Irene A. Stegun. *Handbook of mathematical functions with formulas, graphs, and mathematical tables*, volume No. 55 of *National Bureau of Standards Applied Mathematics Series*. U. S. Government Printing Office, Washington, DC, 1964. For sale by the Superintendent of Documents.

[Bau24]   Peter Bauer. What if? numerical weather prediction at the crossroads. *Journal of the European Meteorological Society*, 1:100002, 2024.

[BBC$^+$95]   Adriano Barenco, Charles H. Bennett, Richard Cleve, David P. DiVincenzo, Norman Margolus, Peter W. Shor, T. Sleator, John A. Smolin, and Harald Weinfurter. Elementary gates for quantum computation. *Physical review. A, Atomic, molecular, and optical physics*, 52 5:3457–3467, 1995.

[BC22]   Dominic W. Berry and Pedro C. S. Costa. Quantum algorithm for time-dependent differential equations using dyson series. *Quantum*, 2022.

[BCOW17]   Dominic W. Berry, Andrew M. Childs, Aaron Ostrander, and Guoming Wang. Quantum algorithm for linear differential equations with exponentially improved dependence on precision. *Communications in Mathematical Physics*, 356:1057 – 1081, 2017.

[BL24]   Peter Brearley and Sylvain Laizet. Quantum algorithm for solving the advection equation using hamiltonian simulation. *Physical Review A*, 110, 07 2024.

[BTB15]   Peter Bauer, Alan Thorpe, and Gilbert Brunet. The quiet revolution of numerical weather prediction. *Nature*, 525(7567):47–55, September 2015.

[Car32]   Torsten Carleman. Application de la théorie des équations intégrales linéaires aux systèmes d'équations différentielles non linéaires. *Acta Mathematica*, 59:63–87, 1932.

[CKS15]   Andrew M. Childs, Robin Kothari, and Rolando D. Somma. Quantum algorithm for systems of linear equations with exponentially improved dependence on precision. *SIAM J. Comput.*, 46:1920–1950, 2015.

[CLVBY24]   Daan Camps, Lin Lin, Roel Van Beeumen, and Chao Yang. Explicit Quantum Circuits for Block Encodings of Certain Sparse Matrices. *SIAM J. Matrix Anal. Appl.*, 45(1):801–827, 2024.

[CO21]   Andrew Childs and Aaron Ostrander. High-precision quantum algorithms for partial differential equations. *Quantum*, 5:574, 11 2021.

[CSMB25]   Pedro C. S. Costa, Philipp Schleich, Mauro E. S. Morales, and Dominic W. Berry. Further improving quantum algorithms for non-linear differential equations via higher-order methods and rescaling. *npj Quantum Information*, 11(1):141, August 2025.

[CW12]   Andrew Childs and Nathan Wiebe. Hamiltonian simulation using linear combinations of unitary operations. *Quantum Information and Computation*, 12, 02 2012.

[DMB+25]   Alexander Dalzell, Sam McArdle, Mario Berta, Przemyslaw Bienias, Chi-Fang Chen, András Gilyén, Connor Hann, Michael Kastoryano, Emil Khabiboulline, Aleksander Kubica, Grant Salton, Samson Wang, and Fernando Brandão. *Quantum Algorithms: A Survey of Applications and End-to-end Complexities.* 05 2025.

[DMWL21]   Yulong Dong, Xiang Meng, K. Whaley, and Lin Lin. Efficient phase-factor evaluation in quantum signal processing. *Physical Review A*, 103, 04 2021.

[Dra00]   Thomas G. Draper. Addition on a quantum computer, 2000.

[Eps05]   Charles L. Epstein. How well does the finite Fourier transform approximate the Fourier transform? *Comm. Pure Appl. Math.*, 58(10):1421–1435, 2005.

[GSLW19]   András Gilyén, Yuan Su, Guang Hao Low, and Nathan Wiebe. Quantum singular value transformation and beyond: exponential improvements for quantum matrix arithmetics. In *Proceedings of*

the 51st Annual ACM SIGACT Symposium on Theory of Computing, STOC 2019, page 193–204, New York, NY, USA, 2019. Association for Computing Machinery.

[HHL09]   Aram W. Harrow, Avinatan Hassidim, and Seth Lloyd. Quantum algorithm for linear systems of equations. *Physical Review Letters*, 103(15), oct 2009.

[HJLZ24]   Junpeng Hu, Shi Jin, Nana Liu, and Lei Zhang. Quantum circuits for partial differential equations via schrödingerisation. *Quantum*, 8:1563, 12 2024.

[HO25]   Gard Olav Helle and Anna Bomme Ousager. https://github.com/GOHelle/QC_advection-diffusion_sim, 2025.

[IBP⁺24]   Julia Ingelmann, Sachin Bharadwaj, Philipp Pfeffer, Katepalli Sreenivasan, and Jörg Schumacher. Two quantum algorithms for solving the one-dimensional advection-diffusion equation. *Computers & Fluids*, 281:106369, 07 2024.

[JATK⁺24]   Ali Javadi-Abhari, Matthew Treinish, Kevin Krsulich, Christopher J. Wood, Jake Lishman, Julien Gacon, Simon Martiel, Paul D. Nation, Lev S. Bishop, Andrew W. Cross, Blake R. Johnson, and Jay M. Gambetta. Quantum computing with Qiskit, 2024.

[Kro23]   Hari Krovi. Improved quantum algorithms for linear and nonlinear differential equations. *Quantum*, 7:913, February 2023.

[KWBAG17]   Ian D Kivlichan, Nathan Wiebe, Ryan Babbush, and Alán Aspuru-Guzik. Bounding the costs of quantum simulation of many-body physics in real space. *Journal of Physics A: Mathematical and Theoretical*, 50(30):305301, jun 2017.

[LC16]   Guang Hao Low and Isaac L. Chuang. Hamiltonian simulation by qubitization. *Quantum*, 2016.

[LC17]   Guang Hao Low and Isaac L. Chuang. Optimal hamiltonian simulation by quantum signal processing. *Phys. Rev. Lett.*, 118:010501, Jan 2017.

[LKK⁺21]   Jin-Peng Liu, Herman Kolden, Hari Krovi, Nuno Loureiro, Konstantina Trivisa, and Andrew Childs. Efficient quantum algorithm for dissipative nonlinear differential equations. *Proceedings of the National Academy of Sciences*, 118:e2026805118, 08 2021.

[LKWMK25]   Michael Lubasch, Yuta Kikuchi, Lewis Wright, and Conor Mc Keever. Quantum circuits for partial differential equations in fourier space. *Phys. Rev. Res.*, 7:043326, Dec 2025.

[LNY23]   Haoya Li, Hongkang Ni, and Lexing Ying. On efficient quantum block encoding of pseudo-differential operators. *Quantum*, 7:1031, 06 2023.

[LYC16]   Guang Hao Low, Theodore J. Yoder, and Isaac L. Chuang. Methodology of resonant equiangular composite quantum gates. *Physical Review X*, 6:041067, 2016.

[MRTC21]   John M. Martyn, Zane M. Rossi, Andrew K. Tan, and Isaac L. Chuang. Grand Unification of Quantum Algorithms. *PRX Quantum*, 2(4):040203, December 2021.

[MW24]   Danial Motlagh and Nathan Wiebe. Generalized quantum signal processing. *PRX Quantum*, 5, 06 2024.

[NC10]   Michael A. Nielsen and Isaac L. Chuang. *Quantum Computation and Quantum Information: 10th Anniversary Edition*. Cambridge University Press, 2010.

[NJ24]   Ivan Novikau and Ilon Joseph. Quantum algorithm for the advection-diffusion equation and the Koopman-von Neumann approach to nonlinear dynamical systems. *arXiv e-prints*, page arXiv:2410.03985, October 2024.

[OBB+25]   Paul Over, Sergio Bengoechea, Peter Brearley, Sylvain Laizet, and Thomas Rung. Quantum algorithm for the advection-diffusion equation by direct block encoding of the time-marching operator. *Physical Review A*, 112, 06 2025.

[OM24]   L. Olivetti and G. Messori. Advances and prospects of deep learning for medium-range extreme weather forecasting. *Geoscientific Model Development*, 17:2347–2358, 2024.

[QSS07]   Alfio Quarteroni, Riccardo Sacco, and Fausto Saleri. *Numerical mathematics*, volume 37 of *Texts in Applied Mathematics*. Springer-Verlag, Berlin, second edition, 2007.

[SBW+18]   Thomas C. Schulthess, Peter Bauer, Nils P. Wedi, Oliver Fuhrer, Torsten Hoefler, and Christoph Schär. Reflecting on the goal and baseline for exascale computing: A roadmap based on weather and climate simulations. *Computing in Science & Engineering*, 21(1):30–41, 2018.

[STY+21]   Xiaoming Sun, Guojing Tian, Shuai Yang, Pei Yuan, and Shengyu Zhang. Asymptotically optimal circuit depth for quantum state preparation and general unitary synthesis. *IEEE Transactions on Computer-Aided Design of Integrated Circuits and Systems*, 42:3301–3314, 2021.

[XWY⁺24]   Hao-Nan Xie, Shijie Wei, Fan Yang, Zheng-An Wang, Chi-Tong Chen, Heng Fan, and Gui Long. Probabilistic imaginary-time evolution algorithm based on nonunitary quantum circuits. *Physical Review A*, 109, 05 2024.

[ZW17]   Sisi Zhou and Jingbo Wang. Efficient quantum circuits for dense circulant and circulant like operators. *Royal Society Open Science*, 4:160906, 05 2017.